Transition Metals in Catalysis: From Precious to Practical

Article Collection

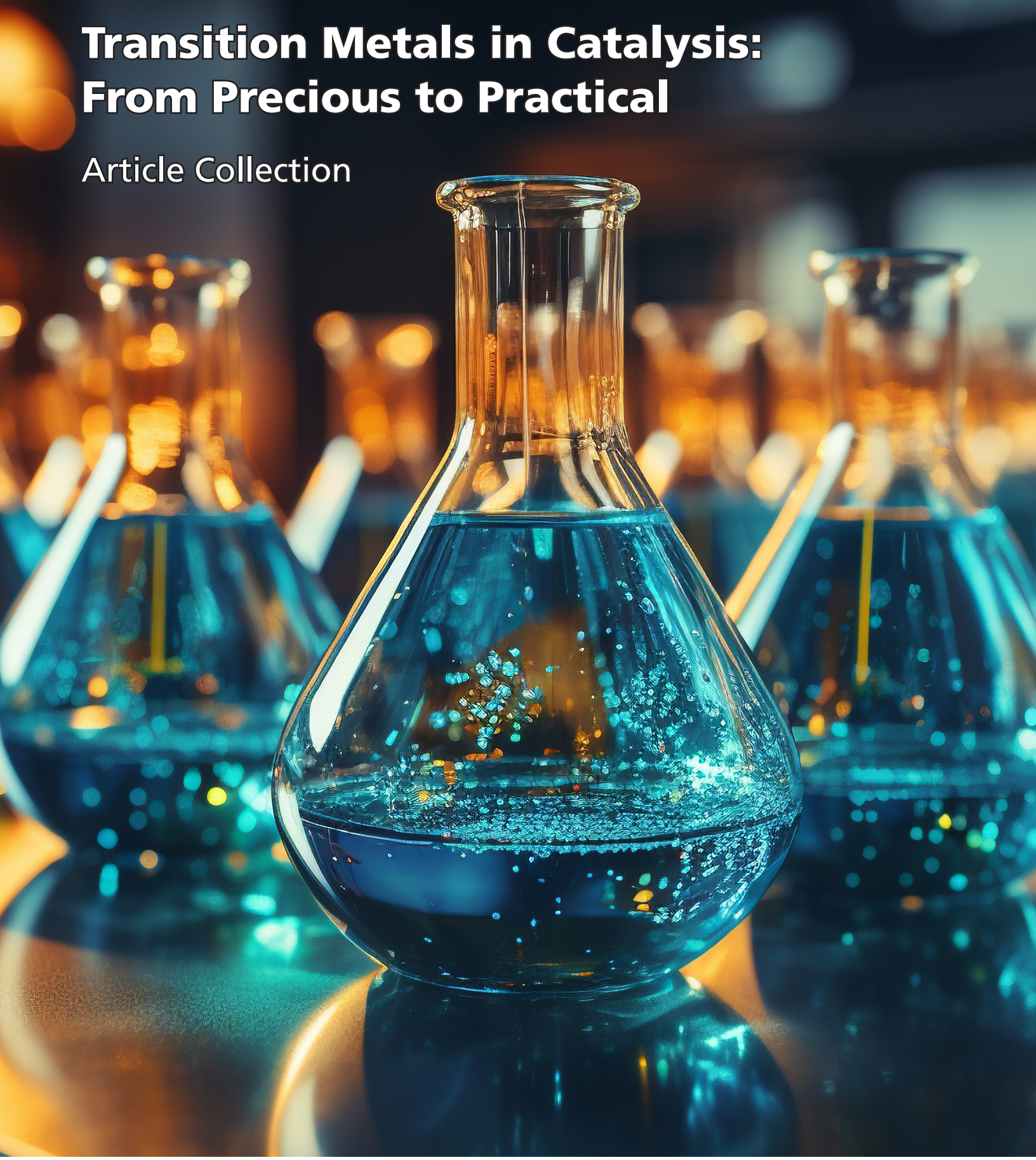

Sponsored by:

WILEY

CHEManager INTERNATIONAL

MERCK

Catalysis from Bench to Production

Explore high-quality catalysts for chemical synthesis. Backed by a robust quality management system and global manufacturing, our chemicals offer a reliable supply chain. Customize orders with QC testing and packaging solutions.

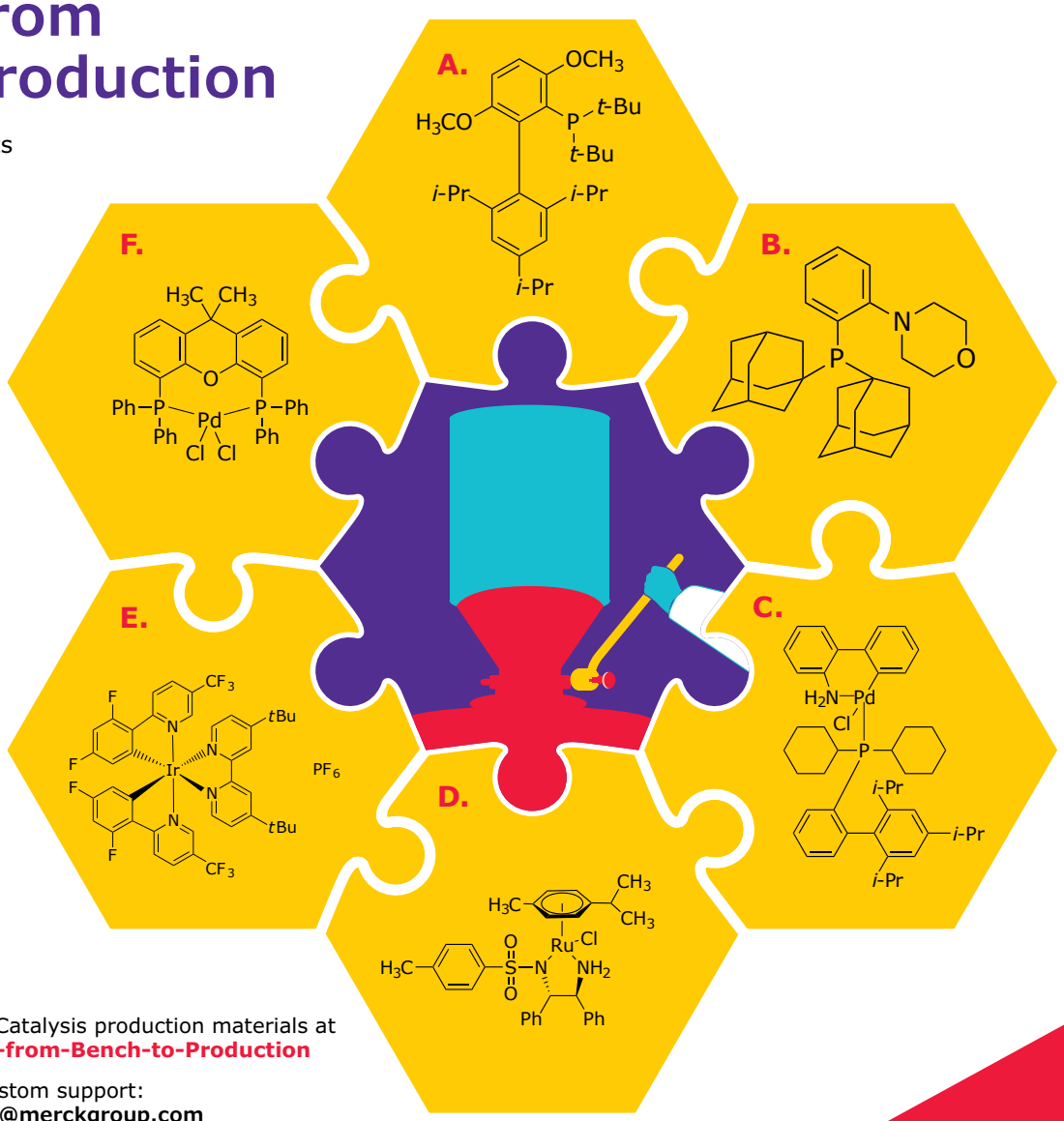

A. Buchwald Ligand = tBuBrettPhos (730998)

B. Non-Buchwald Phosphine Ligand = MorDalPhos (751618)

C. Buchwald & Related Precatalyst = XPhos Pd G2 (741825)

D. Hydrogenation Catalyst = RuCl(p-cymene)[(R,R)-Ts-DPEN] (703907)

E. Photocatalyst = $[Ir\{dF(CF_3)ppy\}_2(dtbpy)]PF_6$ (747793)

F. Metal Salt / Complex = $Pd(XantPhos)Cl_2$ (768146)

View our comprehensive list of Catalysis production materials at **SigmaAldrich.com/Catalysis-from-Bench-to-Production**

Contact us for questions and custom support:
Productionmaterialschemistry@merckgroup.com

MK_AD13156EN 53082 02/2024

The Life Science business of Merck operates as MilliporeSigma in the U.S. and Canada.

Sigma-Aldrich®
Lab & Production Materials

Contents

Introduction

In the dynamic landscape of modern synthetic chemistry, researchers continually push the boundaries of molecular construction. At the heart of this endeavor lies the fascinating realm of catalyzed cross-coupling reactions. These elegant processes allow scientists to stitch together intricate molecular architectures with precision and efficiency. Historically precious metal-based catalysts have been utilized in these transformations; however, the use of first-row transition-metal catalysts has been on the rise. First-row transition metals are abundant, versatile, and catalytically active, and are attractive for industrial applications where cost and sustainability are driving factors. While precious metals retain their allure, it is the first-row transition-metals that drive innovation and shape our molecular landscape. From the interplay of catalysts to the orchestration of diverse substrates, this collection unveils the latest breakthroughs in first-row transition-metal-catalyzed cross-coupling methodologies. These articles illuminate the artistry and innovation inherent in chemical synthesis.

This article collection begins with a study on the development of an iron(III)-catalyzed coupling of thioesters with aliphatic organomanganese reagents. Geiger *et al.* [1] report good functional group tolerance in the successful transformation of a range of thioesters, including biologically relevant compounds. Next, Wang *et al.* [2] describe bench-stable heteroaryl glycosyl sulfones undergoing desulfonylative C–C cross-coupling. The sulfones are coupled with aryl-substituted nucleophiles or electrophiles through two complementary catalytic systems, offering access to a wide variety of C-aryl glycoside products with high diastereoselectivity utilizing iron(II) or nickel(II) catalysis.

Then, Ling *et al.* [3] reports a general copper-catalyzed carbonylative cross-coupling between amines and alkyl iodides. Primary, secondary, and tertiary alkyl iodides were coupled with primary, cyclic and acyclic secondary amines, and anilines in excellent yields. Finally, Chen *et al.* [4] describe the nickel-catalyzed three-component reductive carbonylation of alkyl halides, aryl halides, and ethyl chloroformate. Ethyl chloroformate is utilized as a safe and readily available source of CO, providing an efficient and practical alternative for the synthesis of aryl-alkyl ketones.

Overall first-row transition-metal-catalyzed cross-coupling reactions highlighted show the breadth of possibilities. Traditionally, precious metal-based catalysts have been at the forefront, but now, the spotlight shifts to first-row transition metals—abundant, versatile, and catalytically active. These catalysts are especially useful in industrial applications where cost-effectiveness and sustainability drive innovation. Through the methods and

applications presented in this article collection, we hope to educate researchers on new catalysts and techniques for cross-coupling reactions. To gain a deeper understanding of available options for improving your research, we encourage you to visit Merck's website.

Dr. Christene A. Smith
Editor at CHEManager International

References

[1] Geiger, V.J. *et al.* (2022). Iron-Catalyzed Cross-Coupling of Thioesters and Organomanganese Reagents**. *Chemistry - A European Journal.* DOI: 10.1002/chem.202202212.

[2] Wang, Q. *et al.* (2023). Stereoselective *C*-Aryl Glycosylation by Catalytic Cross-Coupling of Heteroaryl Glycosyl Sulfones. *Angewandte Chemie - International Edition.* DOI: 10.1002/anie.202301081.

[3] Ling, J. *et al.* (2022). Copper-Catalyzed Carbonylative Cross-Coupling of Alkyl Iodides and Amines. *Chemistry - A European Journal.* DOI: 10.1002/chem.202201356.

[4] Chen, H. *et al.* (2022). Reactivity in Nickel-Catalyzed Multi-component Sequential Reductive Cross-Coupling Reactions. *Angewandte Chemie - International Edition.* DOI: 10.1002/anie.202204144.

Chemistry–A European Journal
Research Article
doi.org/10.1002/chem.202202212
Chemistry Europe
European Chemical Societies Publishing

www.chemeurj.org

Iron-Catalyzed Cross-Coupling of Thioesters and Organomanganese Reagents**

Valentin Jacob Geiger,[a] Guillaume Lefèvre,*[b] and Ivana Fleischer*[a]

Dedicated to Prof. Dr. Matthias Beller on the occasion of his 60th birthday

Abstract: We report a Fukuyama-type coupling of thioesters with aliphatic organomanganese reagents utilizing a cheap and easily available iron(III) precatalyst. The reactions exhibit a wide tolerance of solvents and functional groups, allowing for the conversion of thioesters derived from natural products and pharmaceutical compounds. A strong steric impact from each reaction component (carboxylic moiety, thiol substituent and manganese reagent) was displayed, which enabled regioselective transformation of dithioesters. Mechanistic investigations showed that the released thiolate does not act as a mere spectator ligand, but rather positively influences the stability of intermediate alkyl(II)ferrates.

Introduction

The palladium-catalyzed reaction between thioesters and organozinc reagents, generally known as Fukuyama cross-coupling (FCC),[1] constitutes a convenient method for the synthesis of ketones, as demonstrated by several synthetic applications.[2] Besides variations of the palladium catalyst,[3] other transition metals such as the non-precious nickel[4] or cobalt[5] were employed. For the transmetalation step, other less polar reagents such as arylboronic acids introduced by Liebeskind and Srogl[6] or siloxanes reported by Van der Eycken[7] require the presence of stoichiometric amounts of copper in addition to the palladium-based catalysts. To date, couplings using organoboronates,[8] -stannanes[9] and -indium reagents[10] were exclusively developed for palladium-based catalysts. The advantage of using thioesters instead of acid chlorides is their kinetic stability in the presence of water and the possibility to retain the functionality during other synthetic steps, including work-up, which makes them suitable for late-stage functionalizations.

Despite the broad success of organozinc reagents in FCC, the use of attractive non-precious metal catalysts is usually accompanied by limitations regarding the reactivity of organozinc reagents. This was also shown in our work on their Ni-catalyzed coupling with thioesters, wherein aliphatic zinc reagents were completely unreactive, thereby limiting the substrate scope.[4c] Other limitations also occur in Pd-catalyzed reactions, for example the need of stochiometric additives such as Zn(II) salts for the conversion of secondary alkyl reagents.[11] While more reactive Grignard reagents have been shown to resolve the reactivity issue under nonprecious metal catalysis with thioesters[12] or with acid chlorides,[13] the general applicability can be considerably limited. To bridge this gap in reactivity between Grignard and organozinc reagents, we embarked on the employment of organomanganese reagents, which possess a reportedly good functional group tolerance combined with a generally higher reactivity than their zinc analogues (Scheme 1).[14]

In early works, the reactivity of such "manganese Grignard reagents" was mainly studied in non-catalytic reactions or in Cu-

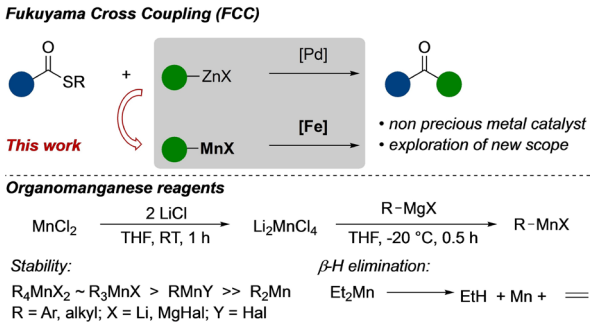

Scheme 1. Fukuyama cross-coupling and our iron-catalyzed coupling of organomanganese reagents.

[a] V. J. Geiger, Prof. Dr. I. Fleischer
Institute of Organic Chemistry
Faculty of Science
Eberhard Karls University Tübingen
Auf der Morgenstelle 18, 72076 Tübingen (Germany)
E-mail: ivana.fleischer@uni-tuebingen.de
Homepage: https://uni-tuebingen.de/de/100267

[b] Dr. G. Lefèvre
i-CLeHS, UMR 8060, CNRS Chimie ParisTech
11, rue Pierre et Marie Curie, 75005 Paris (France)
E-mail: guillaume.lefevre@chimieparistech.psl.eu
Homepage: https://lefevreresearchgroup.com

[**] A previous version of this manuscript has been deposited on a preprint server (https://doi.org/10.26434/chemrxiv.14501436.v1)

Supporting information for this article is available on the WWW under https://doi.org/10.1002/chem.202202212

Chemistry–A European Journal
Research Article
doi.org/10.1002/chem.202202212
Chemistry Europe
European Chemical Societies Publishing

catalyzed couplings.[15] To the best of our knowledge, only limited examples of iron-catalyzed cross-couplings have been reported in this time frame (before 2000).[16] More recent publications contain further examples of inviolate potential of for example aryl manganese compounds or other stabilized manganese reagents in transition metal-catalyzed reactions utilizing Fe or Ni-catalysts.[17] For clarity, the employed reagents can be considered stabilized, since they were unable to undergo β-hydrogen elimination, which is a main decomposition pathway.[18] Another important feature of these reagents is their property to form higher substituted manganates ($LiMnR_3$ or Li_2MnR_4), which led to the recent discovery of a tandem Mn–I exchange/homocoupling, a reactivity thought to be reserved for RLi or RMgX reagents.[19] These literature examples inspire further studies of their so far less known potential, as shown in this work on iron-catalyzed cross-coupling reaction of β-hydrogen containing aliphatic organomanganese reagents with thioesters.

Results and Discussion

On the basis of previous literature, aliphatic manganese reagents were synthesized by treating Grignard reagent with $MnCl_2 \cdot 2$ LiCl.[17a] In the model reaction, thioester **1a** reacted with ethyl manganese bromide lithium chloride complex in the presence of potential catalysts (Table 1). Various transition metal salts provided the product **3aa** in low to moderate yields (Entries 2–6). To our delight, the use of broadly available iron catalysts resulted early on in quantitative conversions and very good yields (Entries 7–10), especially with iron(III) acetylacetonate (acac) (Entry 11). Slightly decreased yield was obtained using only 1 mol% of catalyst, which corresponds to turnover frequency of 516 h^{-1} (Entry 12). The reaction can be performed in almost any ethereal solvent with very good yields as well as in EtOAc (Entries 13–15). Highly polar co-solvents such as *N*-methyl pyrrolidone (NMP) showed a slightly decreased yield (Entry 16). This is in contrast to literature observations in iron-catalyzed Kumada cross-couplings of aryl halides with organomanganese and organomagnesium reagents, which usually perform better with NMP.[16a,c,20] Surprisingly, almost quantitative yields were obtained by using non-degassed THF (Entry 18).

Table 1. Optimization of reaction conditions for the synthesis of octan-3-one.[a]

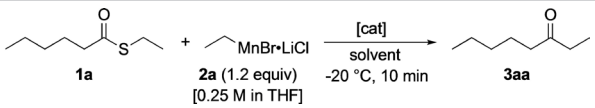

Entry	Catalyst	Solvent[b]	Conv. [%][c]	Yield [%][c]
1	none	THF	18	0
2	$Ni(acac)_2$	THF	95	52
3	$CoCl_2$[d]	THF	81	64
4	CuI[d]	THF	44	37
5	$Pd(PPh_3)Cl_2$	THF	26	18
6	$Mn(acac)_3$	THF	62	5
7	$FeCl_2$[d]	THF	92	82
8	$Fe(acac)_2$	THF	Quant	89
9	$FeCl_3$[d]	THF	Quant	84
10	$(FeCl_3)_2(tmeda)_3$	THF	Quant	89
11	$Fe(acac)_3$	THF	Quant.	91
12	$Fe(acac)_3$[e]	THF	Quant	86
13	$Fe(acac)_3$	THF/Et_2O	Quant	88
14	$Fe(acac)_3$	THF/1,4-dioxane[f]	98	90
15	$Fe(acac)_3$	THF/EtOAc	Quant.	92
16	$Fe(acac)_3$	THF/NMP	90	84
17	$Fe(acac)_3$	THF/DCM	83	71
18	$Fe(acac)_3$	THF[g]	Quant.	98 (78[h])

[a] Reaction conditions: thioester (53.4 mg, 333 µmol, 1 equiv.), EtMnBr·LiCl (400 µmol, 1.2 equiv. based on titre, usually ≤0.28 M in THF), [catalyst] (5 mol%), dry THF (1 mL), −20 °C, 10 min. [b] Mixture: THF/co-solvent = 8:5 (v/v). [c] Determined by quantitative GC-FID using pentadecane as internal standard. [d] 10 mol%. [e] 1 mol%. [f] Slurry due to melting point of the co-solvent. [g] Solvent has not been degassed. [h] Isolated yield.

The performance of organomanganese reagents was more efficient compared to other organometallic compounds under identical reaction conditions (Scheme 2), for example to organozinc reagents, which furnished no product and also to Grignard reagents leading to moderate results and on prolonged reaction period to 1,2-addition. Addition of 10 mol% of $MnCl_2 \cdot 2$ LiCl to a reaction with Grignard reagent did not resolve this issue. Furthermore, a preliminary screening showed an influence of the thioester thiol moiety on the conversion (prim ~ Ar > sec ≫ tert). The 1,2-addition was never observed in the coupling of organomanganese reagents under the applied conditions for standard substrate, even if **3aa** was exposed to the reaction conditions.

Based on this initial screening, a series of *S*-ethyl thioesters was subjected to the coupling with ethyl manganese bromide (Scheme 3). Primary thioesters were converted in good to excellent yields to the products **3ba–fa**, including the sterically demanding 3,3,3-triphenyl substituted substrate **1f**. A strong steric influence on the reaction stems from the α-substitution of the thioester (*prim* > sec_{cyclic} > *tert* > *sec*). The complete breakdown of reactivity of the secondary substrate **1g** and similar aliphatic compounds contrasted with other secondary thioesters having an α-methyl group (**1k**), an α-phenyl group (**1j**) or being cyclic (**1h**, **1i**, **1l**, **1m**), which all underwent the transformation with moderate to excellent yields. The conducted experiments showed that the unreactive **1g** did not poison or slow down the conversion of primary thioester **1b**, yet, **1j** did.

The reaction performed well on a higher scale as exemplified for **3ba**. The diastereomeric ratio of **1h**, **1l** and **1m** (as pure *endo* diastereomer or 5:3 *endo:exo* mixture) remained unchanged.

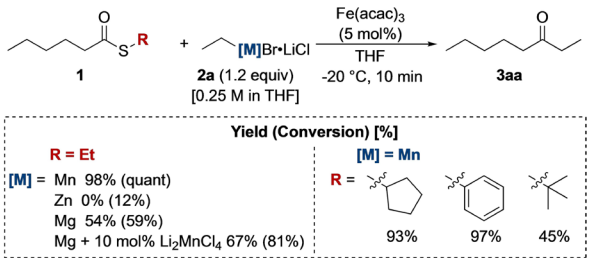

Scheme 2. Iron-catalyzed Fukuyama cross-coupling with different transmetalating reagents and varying *S*-substituents.

Chemistry–A European Journal
Research Article
doi.org/10.1002/chem.202202212
Chemistry Europe
European Chemical Societies Publishing

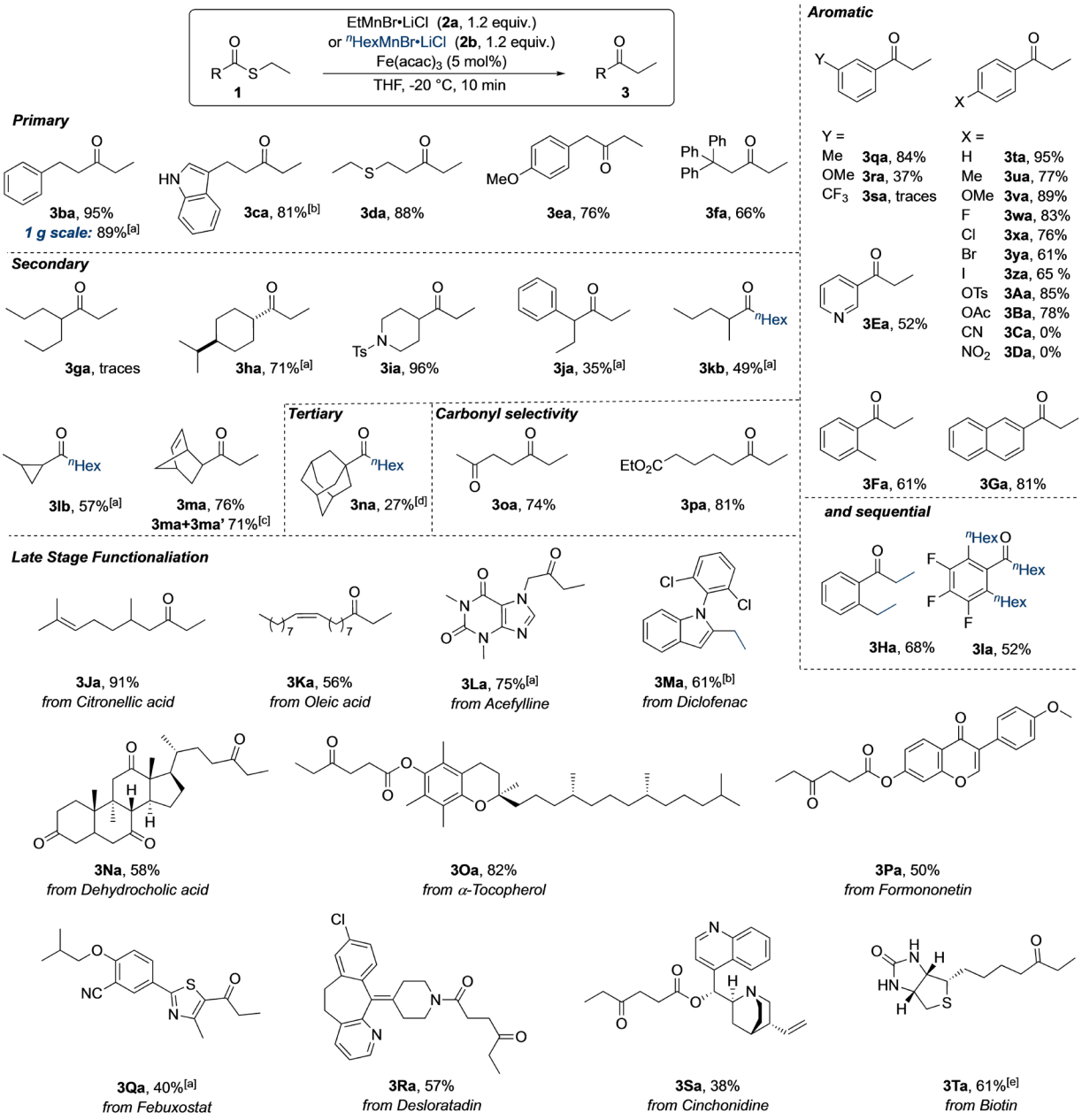

Scheme 3. Coupling of various thioesters with ethyl manganese bromide. Isolated yields are given unless stated otherwise. Standard reaction conditions: thioester (1 mmol, 1 equiv.), EtMnBr·LiCl or ^{n}HexMnBr·LiCl (1.2 mmol, 1.2 equiv. based on titre, usually ≤0.3 M in not degassed THF), $Fe(acac)_3$ (17.7 mg, 50 µmol, 0.05 equiv.), dry THF (1 mL, not degassed), −20 °C, 10 min. [a] 15 min. [b] EtMnBr·LiCl (2.2 mmol, 2.2 equiv. based on titre, usually ≤0.3 M in THF). [c] Mixture of isomers: *endo*/*exo* = 5:3. [d] NMR yield. [e] EtMnBr·LiCl (3.2 mmol, 3.2 equiv. based on titre, usually ≤0.3 M in THF).

Worth mentioning is the successful synthesis of benzylic ketones **3ea** and **3ja** in good yields without decarbonylation products being detected via GC-MS. This indicates that formation of acyl radicals is unlikely, or their recombination with the metal centre is faster than a potential decarbonylation step. Selectivity towards catalytic conversion of the thioester moiety was observed with substrates containing a keto, ester or amide functionality leading to products **3oa**, **3pa** and **3La** in good yields. In our previous studies on the nickel-catalyzed FCC, we were unable to use benzoic acid derived thioesters.[4c] Gratifyingly, several aromatic thioesters with *o*-, *m*-, and *p*-substituents performed well in the coupling reaction. (Pseudo-)halides were tolerated under the reaction conditions furnishing **3wa**–**Ba** products in fair to good yields showing only traces of side products resulting from the oxidative addition into the C–X bond.

Especially, the tolerance of aryl iodides (**3za**) should be highlighted, since this is usually difficult for palladium-catalyzed cross-coupling reactions due to the competing occurrence of

Chemistry–A European Journal
Research Article
doi.org/10.1002/chem.202202212
Chemistry Europe
European Chemical Societies Publishing

Negishi coupling.[3b] Moreover, similar reactivity in iron-catalyzed sp^2-sp^3-cross-coupling is known for Grignard reagents, though in the presence of NMP.[20b] The reaction does not tolerate highly redox-active functionalities such as nitro-groups. Compounds containing a nitrile-group (e.g. **3Ca**) did not furnish product, which might be attributed to a coordination of the functional group to the active catalyst. This claim was substantiated with the addition of the thioester **1C** to the synthesis of **3aa**, which reduced the yield. A methyl group on the aromatic moiety did not affect the results much, only in the case of the sterically more demanding *ortho*-substituted thioester, a lower yield was obtained for the product **3Fa**. Interestingly, the employed *meta*-substituted benzoic acid thioesters **3ra** and **3sa** resulted in diminished yields, depending on the electronic properties of the substituent. Furthermore, a sequential reactivity was observed for the conversion of thioester derived from *ortho*-fluoro-functionalized benzoic acid yielding **3Ha** and **3Ia**, which formed through concurrent activation of the C–S and C–F bonds. This was found to be applicable to every *ortho*-halide substituted thioester. Similar reactivity was reported in instance of organomanganese reagents with *ortho*-chloro- or bromo-substituted phenones by Cahiez.[21] It should also be noted that heterocyclic cores, which might coordinate to metal and thus hinder the reaction, were tolerated in this case (products **3Ea** and **3ca**).

To explore the suitability of this method for late-stage functionalization, thioesters derived from citronellic acid **1J**, oleic acid **1K**, acefylline **1L**, dehydrocholic acid **1N**, α-tocopherol **1O**, formononetin **1P**, febuxostat **1Q**, desloratadin **1R**, cinochonidine **1S** and biotin **1T** could be converted in moderate to excellent yields. Some of the compounds were converted in a two-step strategy utilizing a linker, in order to extend the scope of suitable targets to amines and alcohols. Upon subjecting Diclofenac thioester **1M** to the reaction conditions, the sequential coupling/enamine formation was observed, leading to a functionalized indole derivative **3Ma**. Notably, no side reaction from the C–Cl bond activation occurred.

In addition, a useful regioselective coupling was demonstrated for sterically differentiated thioester **4** (Scheme 4). A selective mono-coupling of the primary thioester moiety was achieved by using 1.2 equivalents of the transmetalating reagent providing **5** in 62% yield. Whereas 2.2 equivalents of **2a** led to coupling of both thioesters to yield 79% of diketone **6** after slightly longer reaction time.

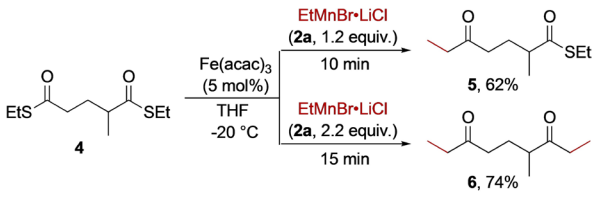

Scheme 4. Selective mono- or double-coupling of dithioester **4**.

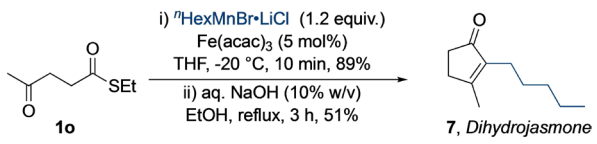

Scheme 5. Synthesis of the natural compound dihydrojasmone.

The reaction was also employed in the synthesis of dihydrojasmone, furnishing the precursor undecane-2,4-dione (**3ob**) in very good yield (Scheme 5). The diketone was then further converted to the natural product **7** by an aldol reaction known from previously described synthesis.[22]

Next, we explored the performance of different organomanganese reagents (Scheme 6). As expected, chain length of non-branched aliphatic organomanganese reagents had only a weak influence on reaction performance, as ketones **3bc** and **3bd** were obtained in very good yields. For the successful synthesis of **3bd** the reagent originated from the organolithium analogue. It can therefore be assumed that the reaction is independent on any Mg(II)-cations from the Grignard precursor. Also, secondary organomanganese reagents **2e** and **2f** were converted with high yields of 90% and 87%. *tert*-Butyl manganese bromide only led to traces of product, which was reasoned by its steric bulk leading to a low reactivity. The homobenzylic ketone **3bg** was obtained in fair yield.

With this in mind, the role of the transmetalating reagent was assumed to be dependent on its ability to undergo β-hydrogen elimination.[18,23] Surprisingly, reactivity was observed with benzyl manganese halide as reagent, although in poor yield and with high amounts of bisbenzyl as homocoupling side product. This is in line with the results from iron-catalyzed cross-coupling of comparable Grignard reagents (Ph, Bn). These usually require a ligand or additive depending on the electronic properties of the coupling compounds.[24] To this end, experiments employing methyl- or phenyl-manganese reagent performed only poorly. The reaction of manganese reagent possessing sterically shielded β-hydrogen atoms yielded only traces of product **3bi** under standard conditions. However, the

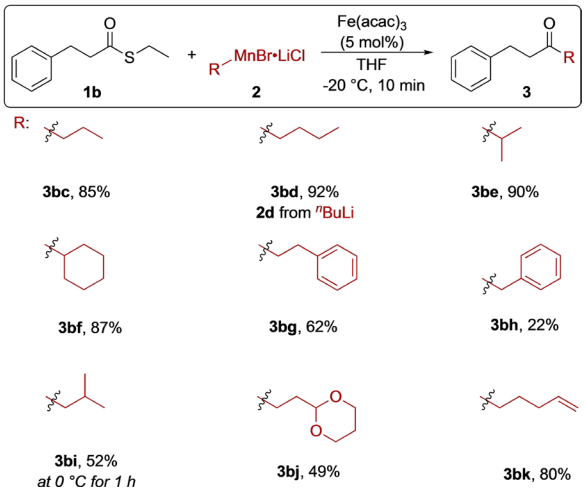

Scheme 6. Variation of the organomanganese reagent in the coupling with thioester **1b**.

Chemistry–A European Journal
Research Article
doi.org/10.1002/chem.202202212
Chemistry Europe
European Chemical Societies Publishing

reaction could be observed at 0 °C for 1 h. Functionalities such as double bond or acetal were tolerated, as demonstrated by the synthesis of **3 bj** and **3 bk**.

Then, we monitored the transformation of three thioesters with varying steric bulk (Figure 1). The conversion of substrate **1 a** was completed in less than 1 min which couldn't be further resolved by lowering the reaction temperature. The reintroduction of additional starting materials after complete reaction led to further conversion.

The strong influence of the substituent at the α-position was confirmed. The reason is possibly the steric interaction with the catalyst, enolization in the case of secondary thioesters and resulting inhibition. To underline the steric effect on tertiary substrates, the reacted solution containing **1 n** was treated with additional precatalyst after 30 minutes and increased conversion was observed (see Supporting Information). The low reactivity of secondary substrates could be resolved by employing more reactive *S*-aryl thioester (Scheme 7).[25] However, in direct comparison with primary thioesters no favoured conversion of *S*-aryl thioester was observed. Interestingly, Cahiez et al. used iron arylthiolate salts as precatalysts of a Kumada coupling of vinyl chlorides.[26] These results contrast the observed formation of disulfides and iron black, when iron salts were exposed to thiolate salts.

In order to gather mechanistic insights into the FCC procedure reported in this work, the behavior of $Fe(acac)_3$ under catalytically relevant conditions (that is, in the presence of an excess of thioester **1 a** and of a nucleophile) was analyzed by paramagnetic ^{1}H NMR. Due to the high paramagnetism of the Mn(II) ion in RMnBr species which prevented efficient NMR analysis of the reaction medium, an aliphatic Grignard reagent (*n*-octylMgBr) was used as a model species. $Fe(acac)_3$ is characterized in THF-d_8 by a well-defined ^{1}H NMR spectrum with two broad resonances at 21 ppm (6H) and −27 ppm (1H).[27] Those signals did not evolve upon addition of 6 equiv. of **1 a**, confirming the necessity of a reduced iron species to activate the thioester. Upon addition of 2 equiv. *n*-octylMgBr (vs. Fe) on a mixture of $Fe(acac)_3$ and 6 equiv. **1 a** after 2 minutes at 20 °C, a new downfielded broad peak appeared at +159 ppm (Figure 2).

In this context, such a highly downfielded broad resonance ($\Delta\nu = 660$ Hz) can be diagnostic of the β-protons of an aliphatic chain borne by a high-spin Fe(II) species ([Fe^{II}]-$CH_2C\underline{H}_2R$; the protons in the α-position being undetected). Similar examples of β-H in high-spin [Fe^{II}]-$CH_2C\underline{H}_2R$ complexes have been reported by Chirik ($\delta = 150$ ppm, $\Delta\nu = 555$ Hz for L$Fe^{II}CH_2C\underline{H}_3$; L = bis(imino)pyridine ligand)[28] or more recently by Werncke ($\delta = 166$ ppm for $[(hmds)_2Fe^{II}CH_2C\underline{H}_2CH_2CH_3]^-$; hmds = N-$(SiMe_3)_2^-$).[29] In our case, the signal observed at 159 ppm quickly disappeared (full disappearance in 5 minutes), and was not observed in the absence of **1 a**. Concomitantly, GC-MS of the reaction medium after hydrolysis confirmed the formation of the coupling product *n*-octylC(O)Pent under these conditions (ca. 60 % vs. *n*-octylMgBr). These results show that alkyliron(II) intermediates can be detected when an iron source reacts with a Grignard reagent in the presence of a thioester. Albeit particularly elusive, the paramagnetic alkyliron(II) species detected in these conditions (Figure 2) displays an enhanced stability compared to what is obtained when $Fe(acac)_3$ is treated by *n*-octylMgBr in the absence of **1 a**. This indeed leads to formation of a dark-brown suspension and to a silent ^{1}H NMR spectrum in the +200/−200 ppm area, which is usually observed when iron salts are reduced in the absence of external stabilizing ligands.[30] Moreover, when **1 a** (10 equiv. vs. Fe) is

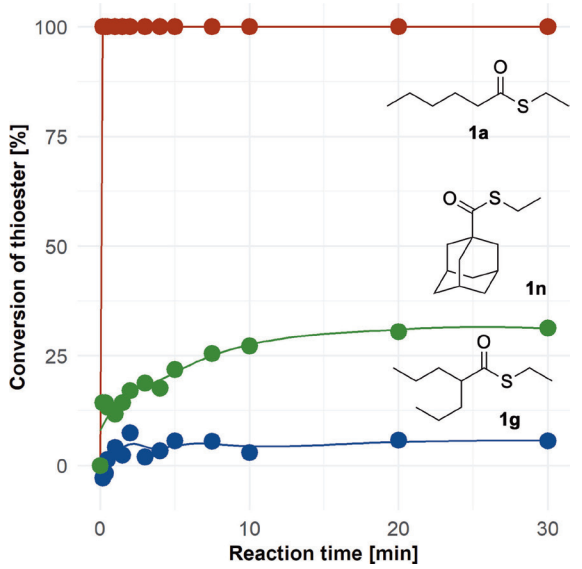

Figure 1. Conversion of different thioesters under catalytic conditions.

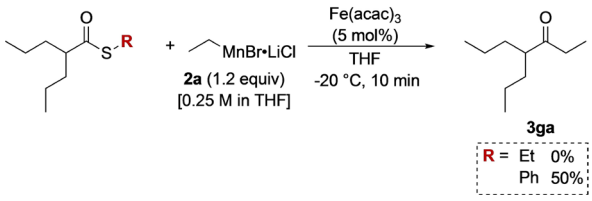

Scheme 7. Improving the reactivity of thioesters by modification of the S-substituent.

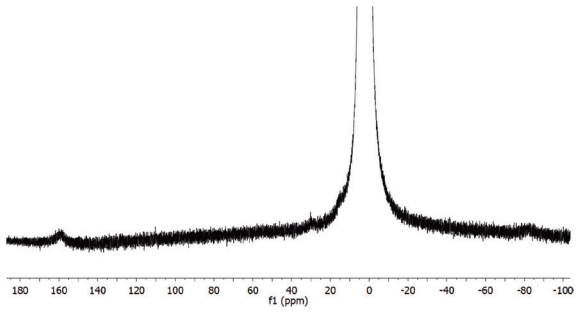

Figure 2. ^{1}H NMR spectrum (60 MHz) of $Fe(acac)_3$ in THF-d_8 in mixture with *n*-octylMgBr (2 equiv.) and **1 a** (6 equiv.) after 2 minutes at 20 °C.

Chemistry–A European Journal
Research Article
doi.org/10.1002/chem.202202212
Chemistry Europe
European Chemical Societies Publishing

added to this suspension, no trace of coupling product is observed, pointing towards the absence of reactivity of a too highly reduced iron species (that is, with an oxidation state lower than +II) in the coupling process.

Importantly, the observation of alkyliron(II) intermediates in conditions allowing the proficiency of the cross-coupling suggests that (i) **1a** or one of its byproducts formed upon the coupling process can play a role in the stabilization of the alkyl-Fe^{II} bond, and (ii) the latter is an on-cycle intermediate of the coupling. Due to the high instability of alkyliron(II) species in the absence of supporting co-ligand at room temperature, and aiming at investigating the reactivity of this oxidation state towards thioesters, we investigated more closely the reactivity of the more thermally stable organoferrous complex $[Fe^{II}(mes)_3]^-$ towards thioester **1a** (mes = 2,4,6-$Me_3C_6H_2$). The former complex is easily detected by its paramagnetic ^{1}H NMR signals at $\delta = 127$ (*meta*-H), 109 (*para*-CH_3) and 26 ppm (*ortho*-CH_3) in a 2/3/6 ratio (Figure 3a).

When $[Fe^{II}(mes)_3]^-$ was treated with 8 equiv. **1a**, the former progressively disappeared while a set of new paramagnetic signals was detected (Figure 3b). Two species **I** and **II** were formed ($\delta_I = 21$ and 16 ppm; $\delta_{II} = 32$, 13.1 and − 2 ppm). After 2 h at 20 °C, no trace of $[Fe^{II}(mes)_3]^-$ was detected in the ^{1}H NMR spectrum, which solely showed **I** and **II** (Figure 3c). Detection of paramagnetic ^{1}H NMR signals in the +30/− 10 ppm area may be indicative of the formation of various mes-Fe^{II} species, with either an intermediate spin ($S = 1$, triplet), as reported by Chirik,[31] or of oligonuclear structures with high-spin Fe^{II} ions ($S = 2$, quintet) which lead to more modest paramagnetic shifts due to antiferromagnetic Fe^{II}-Fe^{II} coupling.[32] Unfortunately, no sample suitable for X-ray diffraction, which could unambiguously assess a structure for **I** or **II**, could be obtained. However, intriguingly, formation of species **I** and **II** was also observed when $[Fe^{II}(mes)_3]^-$ was treated by 0.3 equiv. of EtSMgBr (Figure S4). Since the same distribution of species is obtained when $[Fe^{II}(mes)_3]^-$ is treated by EtSMgBr or by **1a**, along with some coupling product MesC(O)Pent in the latter case, this suggests that the thiolate anions EtS^-, generated at each coupling cycle involving thioester **1a**, are involved in the formation process of species **I** and **II**. These two complexes might thus involve ligation of Fe(II) ions by a combination of mesityl and thiolate anions in a mono- or polynuclear structure. In other words, in terms of reactivity in the FCC context, this means that the thiolate leaving group generated upon coupling of **1a** with the nucleophile (either RMgBr in those mechanistic studies or RMnBr in the FCC scope discussed herein) does not act as a mere spectator anion. Indeed, this shows that thiolate anions can also govern the nature of the distribution of on-cycle Fe(II) species. Ferrous thiolate intermediates can thus be generated progressively in the coupling process, stabilizing the Fe(II) oxidation state and preventing its reductive decomposition towards non-active species. Additionally, **I** and **II** reacted upon addition of 2 equiv. MesMgBr to afford back $[Fe^{II}(mes)_3]^-$, thus confirming their Fe(II) oxidation state (Figure 3d).

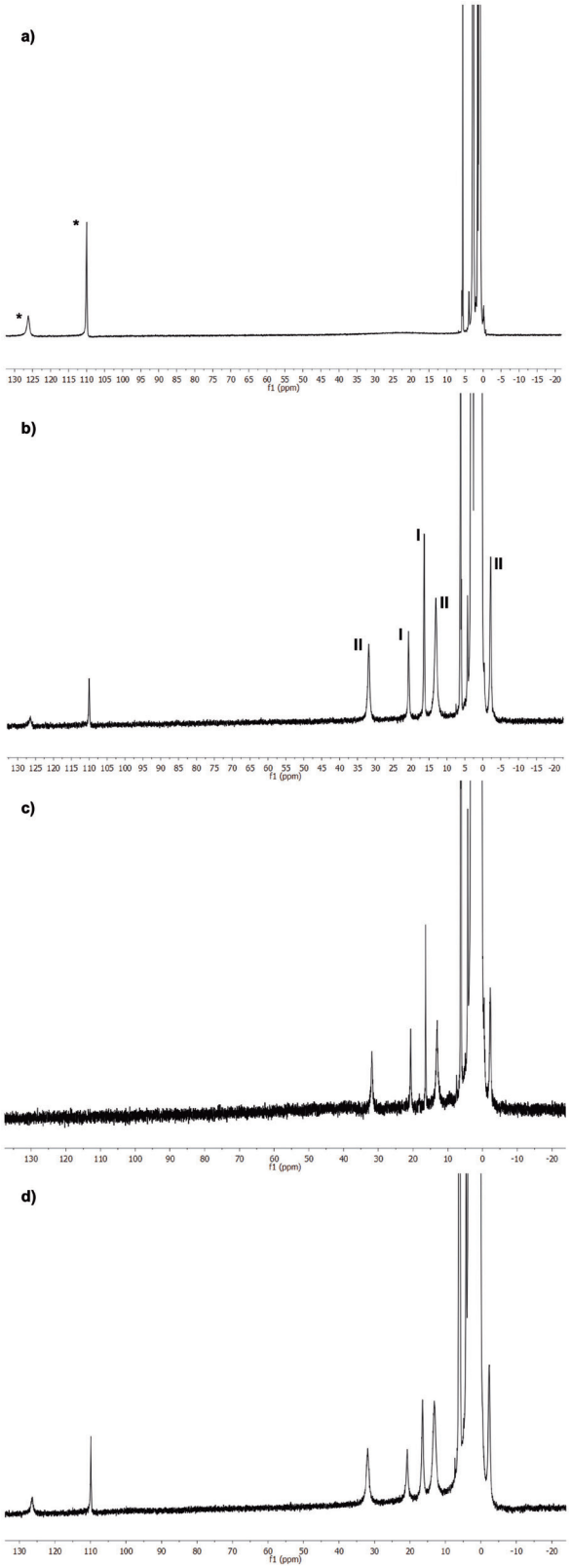

Figure 3. ^{1}H NMR studies of $[Fe(mes)_3]^-$ in THF-d_8: a) Mixture of MesMgBr (3.2 equiv.) and $FeCl_2$ at 20 °C. b) Treatment with **1a** (8 equiv.) after 20 min, c) after 2 h. d) Addition of further MesMgBr (2 equiv.); the starred peaks (*) belong to $[Fe(mes)_3]^-$.

Chemistry–A European Journal
Research Article
doi.org/10.1002/chem.202202212
Chemistry Europe
European Chemical Societies Publishing

Conclusion

In summary, we have developed an iron-catalyzed cross-coupling of thioesters with non-stabilized organomanganese reagents. A range of differently functionalized, natural and pharmaceutical compounds could be converted using the catalytic system. Influences on the reaction yield are determined by the steric demands of the carboxylic and the thiol moiety as well as the organomanganese reagent. Based on this steric dependence, we have demonstrated selective transformation for specific thioester motifs enabling regioselectivity. The low reactivity of some compounds could be lifted by modification of S-substituent. Paramagnetic NMR studies on model compounds gave insights into the possible participation of high spin alkyl iron(II) thiolates.

Acknowledgements

We thank R. Richter, L. Biehler, S. Jeltsch, C. Wilhelm and R. Kern for the synthesis of several compounds as well as for their tenacious endeavours to research facets of this topic that weren't further pursued. Financial support from Boehringer Ingelheim Stiftung (Exploration Grant, I.F.) and the University of Tübingen is gratefully acknowledged. G. L. thanks CNRS for funding the IrMaCAR IRP project. Open Access funding enabled and organized by Projekt DEAL.

Conflict of Interest

The authors declare no conflict of interest.

Data Availability Statement

The data that support the findings of this study are available in the supplementary material of this article. Additional data (e.g. fid files) can be obtained upon request from the authors.

Keywords: cross-coupling · fukuyama · iron catalysis · organomanganese reagents · thioesters

[1] a) H. Tokuyama, S. Yokoshima, T. Yamashita, T. Fukuyama, *Tetrahedron Lett.* **1998**, *39*, 3189–3192; b) H. Tokuyama, S. Yokoshima, T. Yamashita, L. Shao-Cheng, L. Leping, T. Fukuyama, *J. Braz. Chem. Soc.* **1998**, *9*, 381–387; c) V. Hirschbeck, P. H. Gehrtz, I. Fleischer, *Chem. Eur. J.* **2017**, *24*, 7092–7107.
[2] a) M. Seki, M. Hatsuda, Y. Mori, S.-i. Yoshida, S.-i. Yamada, T. Shimizu, *Chem. Eur. J.* **2004**, *10*, 6102–6110; b) H. Ueda, H. Satoh, K. Matsumoto, K. Sugimoto, T. Fukuyama, H. Tokuyama, *Angew. Chem. Int. Ed.* **2009**, *48*, 7600–7603; *Angew. Chem.* **2009**, *121*, 7736–7739; c) D. S. Siegel, G. Piizzi, G. Piersanti, M. Movassaghi, *J. Org. Chem.* **2009**, *74*, 9292–9304; d) S.-Q. Tang, J. Bricard, M. Schmitt, F. Bihel, *Org. Lett.* **2019**, *21*, 844–848; e) J. Talode, D. Kato, H. Nagae, H. Tsurugi, M. Seki, K. Mashima, *J. Org. Chem.* **2020**, *85*, 12382–12392.
[3] a) Y. Mori, M. Seki, *Adv. Synth. Catal.* **2007**, *349*, 2027–2038; b) K. Kunchithapatham, C. C. Eichman, J. P. Stambuli, *Chem. Commun.* **2011**, *47*, 12679–12681; c) A. H. Cherney, S. E. Reisman, *Tetrahedron* **2014**, *70*, 3259–3265.
[4] a) T. Shimizu, M. Seki, *Tetrahedron Lett.* **2002**, *43*, 1039–1042; b) Y. Zhang, T. Rovis, *J. Am. Chem. Soc.* **2004**, *126*, 15964–15965; c) P. H. Gehrtz, P. Kathe, I. Fleischer, *Chem. Eur. J.* **2018**, *24*, 8774–8778.
[5] F. H. Lutter, L. Grokenberger, M. S. Hofmayer, P. Knochel, *Chem. Sci.* **2019**, *10*, 8241–8245.
[6] L. S. Liebeskind, J. Srogl, *J. Am. Chem. Soc.* **2000**, *122*, 11260–11261.
[7] V. P. Mehta, A. Sharma, E. Van der Eycken, *Adv. Synth. Catal.* **2008**, *350*, 2174–2178.
[8] Y. Yu, L. S. Liebeskind, *J. Org. Chem.* **2004**, *69*, 3554–3557.
[9] R. Wittenberg, J. Srogl, M. Egi, L. S. Liebeskind, *Org. Lett.* **2003**, *5*, 3033–3035.
[10] B. W. Fausett, L. S. Liebeskind, *J. Org. Chem.* **2005**, *70*, 4851–4853.
[11] R. Oost, A. Misale, N. Maulide, *Angew. Chem. Int. Ed.* **2016**, *55*, 4587–4590; *Angew. Chem.* **2016**, *128*, 4663–4666.
[12] a) C. Cardellicchio, V. Fiandanese, G. Marchese, L. Ronzini, *Tetrahedron Lett.* **1985**, *26*, 3595–3598; b) W. Oppolzer, C. Darcel, P. Rochet, S. Rosset, J. De Brabander, *Helv. Chim. Acta* **1997**, *80*, 1319–1337.
[13] B. Scheiper, M. Bonnekessel, H. Krause, A. Fürstner, *J. Org. Chem.* **2004**, *69*, 3943–3949.
[14] G. Cahiez, C. Duplais, J. Buendia, *Chem. Rev.* **2009**, *109*, 1434–1476.
[15] a) G. Cahiez, D. Bernard, J. F. Normant, *Synthesis* **1977**, *1977*, 130–133; b) G. Cahiez, J. F. Normant, *Tetrahedron Lett.* **1977**, *18*, 3383–3384; c) G. Cahiez, A. Alexakis, J. F. Normant, *Synth. Commun.* **1979**, *9*, 639–645; d) G. Cahiez, *Tetrahedron Lett.* **1981**, *22*, 1239–1242; e) G. Cahiez, M. Alami, *Tetrahedron Lett.* **1989**, *30*, 3541–3544; f) G. Cahiez, M. Alami, *Tetrahedron Lett.* **1990**, *31*, 7423–7424.
[16] a) G. Cahiez, S. Marquais, *Pure Appl. Chem.* **1996**, *68*, 53–60; b) G. Cahiez, P.-Y. Chavant, E. Metais, *Tetrahedron Lett.* **1992**, *33*, 5245–5248; c) G. Cahiez, S. Marquais, *Tetrahedron Lett.* **1996**, *37*, 1773–1776.
[17] a) A. D. Benischke, A. Desaintjean, T. Juli, G. Cahiez, P. Knochel, *Synthesis* **2017**, *49*, 5396–5412; b) M. S. Hofmayer, J. M. Hammann, G. Cahiez, P. Knochel, *Synth. Lett.* **2018**, *29*, 65–70; c) A. Desaintjean, S. Belrhomari, L. Rousseau, G. Lefèvre, P. Knochel, *Org. Lett.* **2019**, *21*, 8684–8688; d) L. Rousseau, A. Desaintjean, P. Knochel, G. Lefèvre, *Molecules* **2020**, *25*, 723.
[18] M. Tamura, J. Kochi, *J. Organomet. Chem.* **1971**, *29*, 111–129.
[19] M. Uzelac, P. Mastropierro, M. de Tullio, I. Borilovic, M. Tarrés, A. R. Kennedy, G. Aromí, E. Hevia, *Angew. Chem. Int. Ed.* **2021**, *60*, 3247–3253; *Angew. Chem.* **2021**, *133*, 3284–3290.
[20] a) G. A. Molander, B. J. Rahn, D. C. Shubert, S. E. Bonde, *Tetrahedron Lett.* **1983**, *24*, 5449–5452; b) A. Fürstner, A. Leitner, *Angew. Chem. Int. Ed.* **2002**, *41*, 609–612; *Angew. Chem.* **2002**, *114*, 632–635.
[21] G. Cahiez, D. Luart, F. Lecomte, *Org. Lett.* **2004**, *6*, 4395–4398.
[22] W. Y. Lee, Y. S. Lee, S. Y. Jang, S. Y. Lee, *Bull. Korean Chem. Soc.* **1991**, *12*, 26–31.
[23] A. Fürstner, A. Leitner, M. Méndez, H. Krause, *J. Am. Chem. Soc.* **2002**, *124*, 13856–13863.
[24] a) T. Parchomyk, S. Demeshko, F. Meyer, K. Koszinowski, *J. Am. Chem. Soc.* **2018**, *140*, 9709–9720; b) S. B. Muñoz, S. L. Daifuku, J. D. Sears, T. M. Baker, S. H. Carpenter, W. W. Brennessel, M. L. Neidig, *Angew. Chem. Int. Ed.* **2018**, *57*, 6496–6500; *Angew. Chem.* **2018**, *130*, 6606–6610.
[25] Y. Tian, L. Wang, H.-Z. Yu, *RSC Adv.* **2016**, *6*, 61996–62004.
[26] G. Cahiez, O. Gager, J. Buendia, C. Patinote, *Chem. Eur. J.* **2012**, *18*, 5860–5863.
[27] Z. Xue, J.-C. Daran, Y. Champouret, R. Poli, *Inorg. Chem.* **2011**, *50*, 11543–11551.
[28] R. J. Trovitch, E. Lobkovsky, P. J. Chirik, *J. Am. Chem. Soc.* **2008**, *130*, 11631–11640.
[29] C. G. Werncke, J. Pfeiffer, I. Müller, L. Vendier, S. Sabo-Etienne, S. Bontemps, *Dalton Trans.* **2019**, *48*, 1757–1765.
[30] R. B. Bedford, P. B. Brenner, E. Carter, P. M. Cogswell, M. F. Haddow, J. N. Harvey, D. M. Murphy, J. Nunn, C. H. Woodall, *Angew. Chem. Int. Ed.* **2014**, *53*, 1804–1808; *Angew. Chem.* **2014**, *126*, 1835–1839.
[31] E. J. Hawrelak, W. H. Bernskoetter, E. Lobkovsky, G. T. Yee, E. Bill, P. J. Chirik, *Inorg. Chem.* **2005**, *44*, 3103–3111.
[32] a) H. Müller, W. Seidel, H. Görls, *Z. Anorg. Allg. Chem.* **1996**, *622*, 1968–1974; b) A. Klose, E. Solari, C. Floriani, A. Chiesi-Villa, C. Rizzoli, N. Re, *J. Am. Chem. Soc.* **1994**, *116*, 9123–9135.

Manuscript received: July 15, 2022
Accepted manuscript online: July 23, 2022
Version of record online: September 1, 2022

Transition-Metal Catalysis

Stereoselective *C*-Aryl Glycosylation by Catalytic Cross-Coupling of Heteroaryl Glycosyl Sulfones

*Quanquan Wang[+], Boon Chong Lee[+], NingXi Song, and Ming Joo Koh**

Abstract: Stereoselective *C*-glycosylation reactions are increasingly gaining attention in carbohydrate chemistry because they enable glycosyl precursors, readily accessible as anomeric mixtures, to converge to a single diastereomeric product. However, controlling the stereochemical outcome through transition-metal catalysis remains challenging, and methods that leverage bench-stable heteroaryl glycosyl sulfone donors to facilitate glycosylation are rare. Herein, we show two complementary nonprecious metal catalytic systems, based on iron or nickel, which are capable of promoting efficient C–C coupling between heteroaryl glycosyl sulfones and aromatic nucleophiles or electrophiles through distinct mechanisms and modes of activation. Diverse *C*-aryl glycosides were secured with excellent selectivity, scope, and functional-group compatibility, and reliable access to both α and β isomers was possible for key sugar residues.

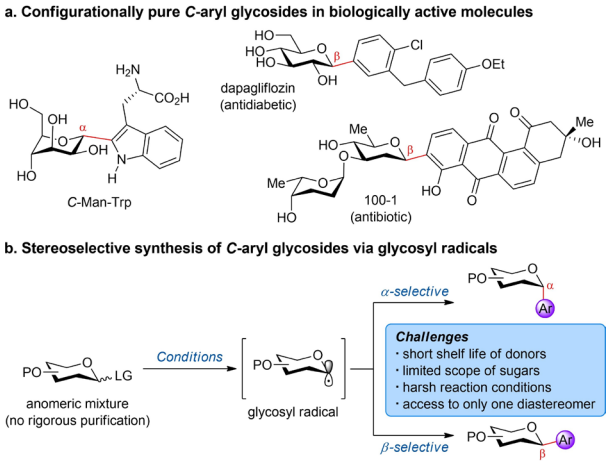

Scheme 1. Bioactive *C*-aryl glycosides and strategies to access them via glycosyl radical species.

Introduction

Stereochemically pure *C*-aryl glycosides are prevalent in biologically active natural products and drugs[1–6] (Scheme 1a). These cyclic saccharides predominantly exist either in their α or β isomeric form, in which the stereochemical identity depends on the configuration at the aryl-substituted C1 (anomeric carbon) center.[2] A classic example of an α-anomeric compound is *C*-mannosyl tryptophan (*C*-Man-Trp),[7–11] which is produced by post-translational protein modification and implicated in key biological pathways, although its functions remain unclear owing to insufficient material to carry out meaningful studies. On the other hand, a number of pharmaceutical agents, such as antidiabetic dapagliflozin[12] and antibiotic 100–1,[13] contain β-anomeric cores. The stability of *C*-aryl glycosidic bonds towards hydrolytic enzymes in vivo has played a paramount role in the design of sugar-based therapeutic candidates as robust surrogates of native *O*-glycosides.[3,6]

Given the significant biological and medicinal value of *C*-aryl glycosides, developing synthetic methodologies that provide efficient access to these entities with high diastereoselectivity is a compelling objective in carbohydrate research.[3,14–18] Particularly desirable is a set of broadly applicable protocols that harness the power of nonprecious base metal catalysis[3,18,19] to transform a readily available glycosyl precursor (donor), the saccharide component which bears a reactive functional group at the C1 position, into the *C*-aryl glycoside product by controlling the stereochemical outcome of C-aryl bond formation.[18] In this regard, processes that convert glycosyl donors into glycosyl radical intermediates[16,17,20–23] en route to *C*-aryl glycosides are highly attractive (Scheme 1b), given that such glycosyl radical cross-coupling reactions are less susceptible to undesired epimerization and elimination side reactions.[16] In contrast to stereospecific transformations,[24–26] the stereochemical purity of the donor is inconsequential, since both α and β isomers eventually converge to a single diastereomeric product, which means that anomeric mixtures of the substrate can be employed without rigorous purification. In most reported methodologies, however, just one diastereomer can be accessed.

Although various glycosyl precursors have been conceived for radical-based *C*-aryl glycosylation over the years,[3,17] donors that are stable in air and yet sufficiently reactive under mild conditions are noticeably rare. For instance, many glycosyl donors derived from 2-deoxgenated[27–29] and unprotected[30] sugars are prone to decomposition under established (harsh) reaction conditions, consequently limiting their utility in practice. These

[*] Dr. Q. Wang,[+] B. C. Lee,[+] N. Song, Prof. Dr. M. J. Koh
Department of Chemistry, National University of Singapore
4 Science Drive 2,Singapore, 117544 (Republic of Singapore)
E-mail: chmkmj@nus.edu.sg

[+] These authors contributed equally to this work.

problems led us to bench-stable heteroaryl glycosyl sulfones,[31,32] of which a diverse spectrum of carbohydrate residues can be readily prepared and dispensed on large scale.[33] Under transition-metal-free photoinduced conditions, these sulfones were found to undergo desulfonylative coupling with activated π-bonds and electrophiles to furnish certain classes of glycosides through glycosyl radical addition/elimination pathways[34] (Scheme 2a). Despite these advances, severe limitations in the range of accessible saccharides still exist, since reactions with less-activated aryl-substituted reagents leading to *C*-aryl glycosides were unsuccessful.[34]

Therefore, there is an urgent demand to develop transformations that fully leverage heteroaryl glycosyl sulfones as a general class of donors for stereoselective *C*-aryl glycosylation, exhibiting high functional-group tolerance with respect to the scope of the sugar residue and aryl moiety. To achieve this, we envisioned that an appropriate base metal catalyst can be exploited to activate the aromatic reaction partner, in order to promote efficient desulfonylative C–C cross-coupling with the sulfone. A potential complication that may arise is the site selectivity of sulfone activation, since transition metals are known to insert into C(sp^2)–S bonds within aryl/alkenyl sulfones[35–37] leading to undesired products. Herein, we disclose a series of versatile Fe- or Ni-catalyzed transformations that address the aforementioned challenges (Scheme 2b).

Results and Discussion

We focused on developing conditions that promote the cross-coupling of heteroaryl glycosyl sulfones (isolated on multi-gram scale and stored under ambient conditions over months) with both aryl nucleophiles and electrophiles, which would enable access to a wider range of *C*-aryl glycoside products. After an extensive survey of various reaction parameters (see Supporting Information section 3 for details), 5 mol % of ligand-free $FeBr_2$ was identified as the optimal catalyst to mediate efficient desulfonylative arylation of 2-pyridyl sulfone **1** (derived from D-mannose) using $Ph_2Zn(tmeda)\cdot 2MgBrCl$ (1.5 equiv) as the nucleophilic reagent in THF at room temperature, delivering *C*-aryl glycoside **2** in 95 % (98 % NMR) yield as a single α isomer (Scheme 3, conditions A). 2-Pyridyl sulfinate salt[38] was also detected as a by-product. These conditions compare favorably with a previous protocol[39] that relied on the use of a complex and sterically encumbered bisphosphine-iron catalyst to carry out arylation at 0 °C. Addition of exogenous ligands or changing the nature of the phenyl nucleophile, iron complex or solvent led to inferior results (see Supporting Information Tables S2–6). **1** was recovered when the reaction was conducted in the absence of $FeBr_2$ or the zinc reagent, suggesting that successful sulfone activation required both components. Cross-coupling with $FeBr_2$ and tmeda as ligand was less efficient (see Supporting Information Table S6), implying that adventitious dissociation of tmeda from the zinc reagent and formation of a tmeda-iron species were unlikely.

On the other hand, 10 mol % of the Ni-based complex derived from $Ni(ClO_4)_2\cdot 6H_2O$ and 4,4′,4″-tri-*tert*-butyl-2,2′:6′,2″-terpyridine (tBu$_3$-terpy) was found to mediate the union of 2-benzothiazolyl sulfone **3** (derived from D-ribose) and 4-iodoanisole in the presence of Zn as reductant and DMSO as solvent to furnish *C*-aryl glycoside **4** in 72 % (78 % NMR) yield as β isomer exclusively at 50 °C (Scheme 3, conditions B). Use of the more reactive 2-benzothiazolyl sulfone (vs. 2-pyridyl variant) was necessary for improved efficiency. It is worth mentioning that 2-benzothiazolyl sulfinate was not observed as a by-product. Instead, substantial amounts of benzothiazole and 2,2′-bibenzothiazole were detected, indicating a distinct sulfone activation mode[40] (see Scheme 5b). Switching/excluding the reductant, replacing the aryl iodide with other electrophiles, or changing the Ni complex/ligand led to diminished efficiency (see Supporting Information Table S9). **4** was isolated in low yield when the reaction was repeated with a

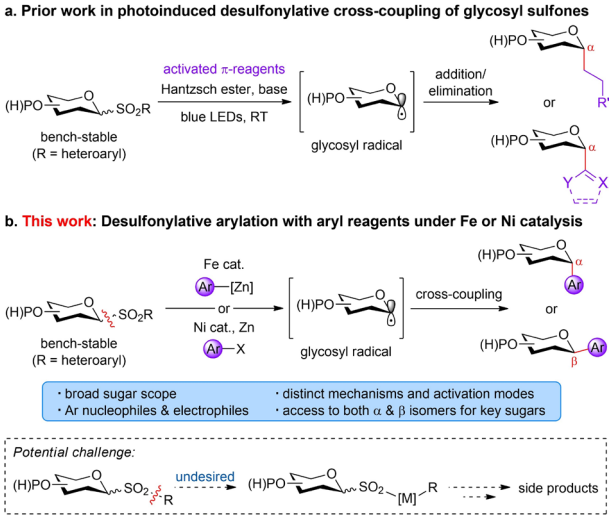

Scheme 2. Heteroaryl glycosyl sulfones as practical donors for stereoselective *C*-aryl glycosylation.

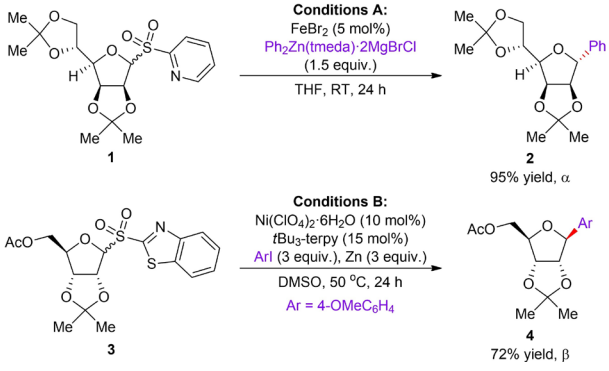

Scheme 3. Optimized conditions for desulfonylative arylation. Reported yields are for isolated and purified products. α:β ratios were determined by ^{1}H NMR analysis.

separately synthesized ArZnI (Ar = 4-OMeC$_6$H$_4$) in place of 4-iodoanisole and Zn, intimating that the present system is less likely to proceed via an aryl zinc species generated in situ. The results in Scheme 3 highlight the versatility of base metal catalysis in facilitating stereoselective desulfonylative arylation under redox-neutral or cross-electrophile coupling settings.

The scope of Fe-catalyzed desulfonylative arylation under conditions A (Table 1) was evaluated by examining different functionalized diaryl zinc nucleophiles as well as 2-pyridyl sulfones prepared from various sugar residues. Diaryl zinc reagents with electronically and/or sterically diverse (hetero)aryl moieties underwent successful C–C coupling with **1**, furnishing *C*-aryl glycosides **5**–**14** solely as α isomers in 49–92 % yield. These include products with functionalizable C(sp^2)–Cl bonds (**8**, **9**) as well as heteroarenes (**12**–**14**). Cyclic and acyclic alkenyl motifs could also be incorporated, affording the corresponding stereodefined *C*-alkenyl glycosides (**15**, **16**).

A variety of pyranose- and furanose-derived 2-pyridyl sulfones also participated in arylation, delivering **17**–**26** in 60–93 % yield with good diastereocontrol. Compared to reported Fe-catalyzed *C*-aryl glycosylation systems that employed less-stable glycosyl halides,[39] bench-stable sulfones obtained from a significantly broader range of saccharides including unprotected (**23**) and 2-deoxysugars (**24**–**26**) could be transformed into the desired *C*-aryl glycoside products.

We next assessed the generality of Ni-catalyzed desulfonylative arylation under conditions B (Table 2) by screening various substituted (hetero)aryl iodides and 2-benzothiazolyl glycosyl sulfones (see Supporting Information Figure S10 for more examples). Similar to the cases in Table 1, varying the electronic and/or steric effects of the electrophilic aryl substituent did not have an appreciable impact on reaction efficiency, and complete β selectivity was observed across the board for the arylation of **3** to afford *C*-nucleoside[6,41] derivatives **27**–**34** in 63–86 % yield. β-**34**, an intermediate of β-RFAP[42] which contains an acidic acetanilide, was readily secured in 86 % yield.

In contrast to a number of Ni-catalyzed protocols[21,43] that suffer from limitations in the scope of pyranoses accessible, our system involving 2-benzothiazolyl sulfones is broadly applicable to both pyranoses (**35**–**40**) and furanoses (**27**–**34**, **41**, **42**). Across the board, high diastereoselectivity could be reliably achieved. Synthesis of peptide-derived **40**

Table 1: Fe-catalyzed desulfonylative arylation with diaryl zinc reagents.

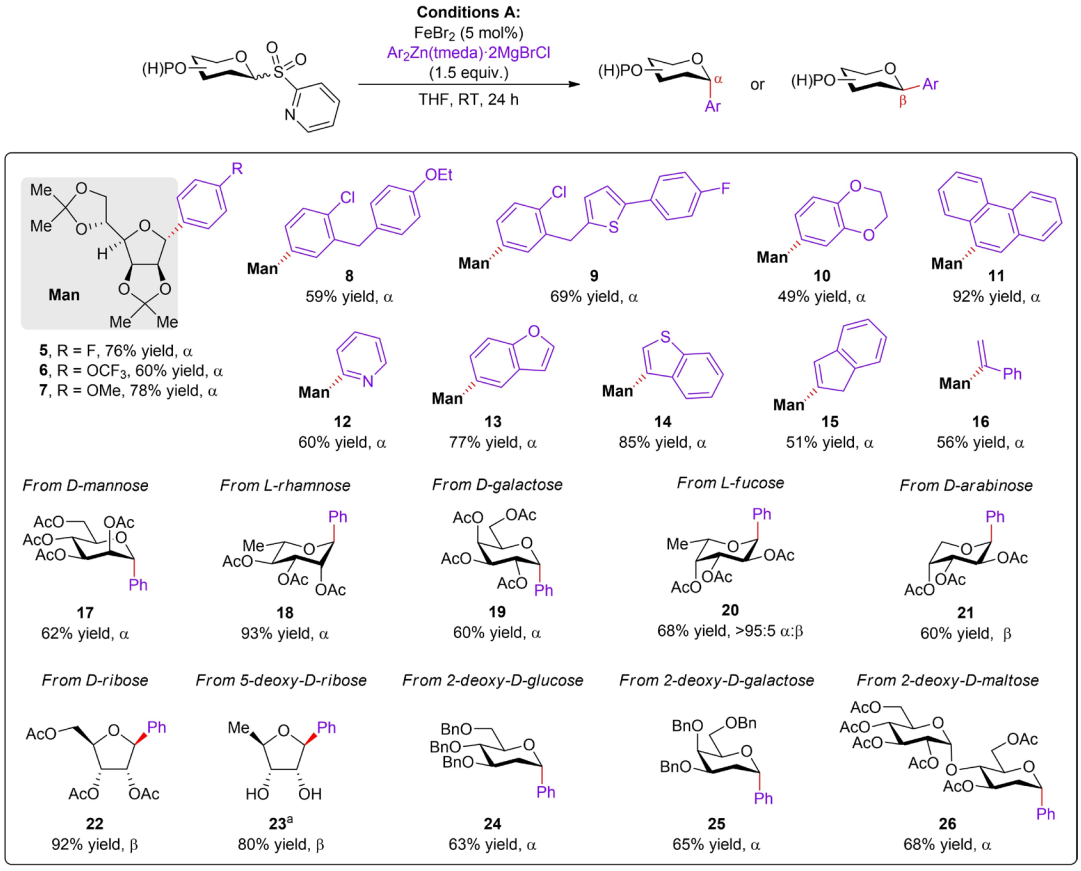

Unless otherwise stated, reported yields are for isolated and purified products. α:β ratios were determined by ^{1}H NMR analysis. [a]The reaction was conducted with Ph$_2$Zn(tmeda)·2MgBrCl (4 equiv). See the Supporting Information for details.

Table 2: Ni-catalyzed desulfonylative arylation with aryl iodides.

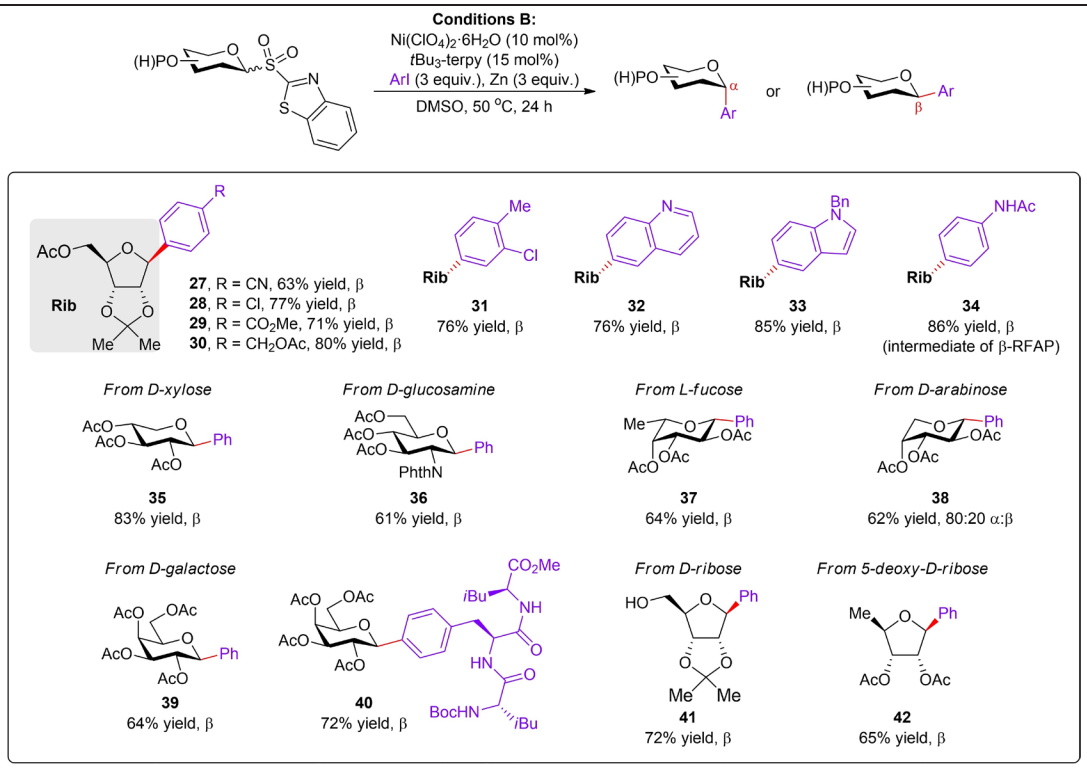

Unless otherwise stated, reported yields are for isolated and purified products. α:β ratios were determined by ^{1}H NMR analysis. See the Supporting Information for details.

(with multiple acidic sites) and free-hydroxy-containing **41** further underscores the functional-group compatibility of the method, and rules out any involvement of a Brønsted basic aryl zinc species.[44] An extended reaction scope is shown in Supporting Information section 4.

Although the exact origin of diastereocontrol in the two desulfonylative arylation regimes is intricate and beyond the scope of this paper, simplified guiding principles could be formulated on the basis of mechanistic nuances associated with the D-glucopyranosyl radical intermediate as a model (Scheme 4a). Previous studies by Nakamura[39] and Giese[45] revealed that this radical exists predominantly in its $B^{2,5}$ boat conformation (slightly more stable than chair-like conformers), and that the radical at C1 has *p*-character (planar carbon center). This means that α- and β-attack could potentially occur to deliver both stereoisomers of the product through C– C coupling, which is probably why poor selectivity was detected for *C*-glucosides in some catalytic manifolds.[16]

Under conditions A, we reasoned that an aryl iron species generated in situ is likely to react faster from the α-face of the $B^{2,5}$ conformer, owing to stabilizing orbital interactions between the ring oxygen and the newly formed C1– Fe bond in the transition state (kinetic anomeric effect[17, 39]). Moreover, the resulting alkyliron **I** adopts a chair-like conformation and is stabilized by the metallo-anomeric effect[46] (donation of electron density from ring oxygen into the C1–Fe σ* antibonding orbital). This presumably overrides any steric repulsion between the axial C1–Fe bond and the neighboring C2 alkoxy group (*cis* relationship), which is further alleviated by the relatively long C1–Fe bond.[47] The ensuing stereoretentive reductive elimination affords **II** in high α selectivity.

In contrast, under conditions B, an aryl nickel species generated in situ bearing a sizeable tridentate *t*Bu$_3$-terpy ligand probably prefers to react from the β-face of the $B^{2,5}$ conformer as it transits towards **III** (equatorial C1–Ni bond and the C2 alkoxy group in a *trans* relationship),[48] outcompeting the inherent stereoelectronic effects. In this case, attack from the opposite face (to form **IV**) would risk severe steric clash with the C2 alkoxy, which is exacerbated by the shorter C1–Ni bond (vs. C1–Fe bond).[47] Following stereoretentive reductive elimination, **V** is secured in high β (1,2-*trans*) selectivity.[49] Overall, the stereochemical outcomes observed in Tables 1 and 2 could be reasonably rationalized by these mechanistic deliberations.

Of particular note, our two complementary catalytic methods offer stereodivergent access to both α and β isomers of *C*-aryl glycosides for a number of common monosaccharide feedstocks (Scheme 4b). Fe-catalyzed cross-coupling led to **19**, **20** and **21**, whereas Ni-catalyzed cross-coupling predominantly gave the opposite diastereomers **39**, **37** and **38**, respectively. However, stereodivergence could not be attained for sugar residues in which stereoelectronic

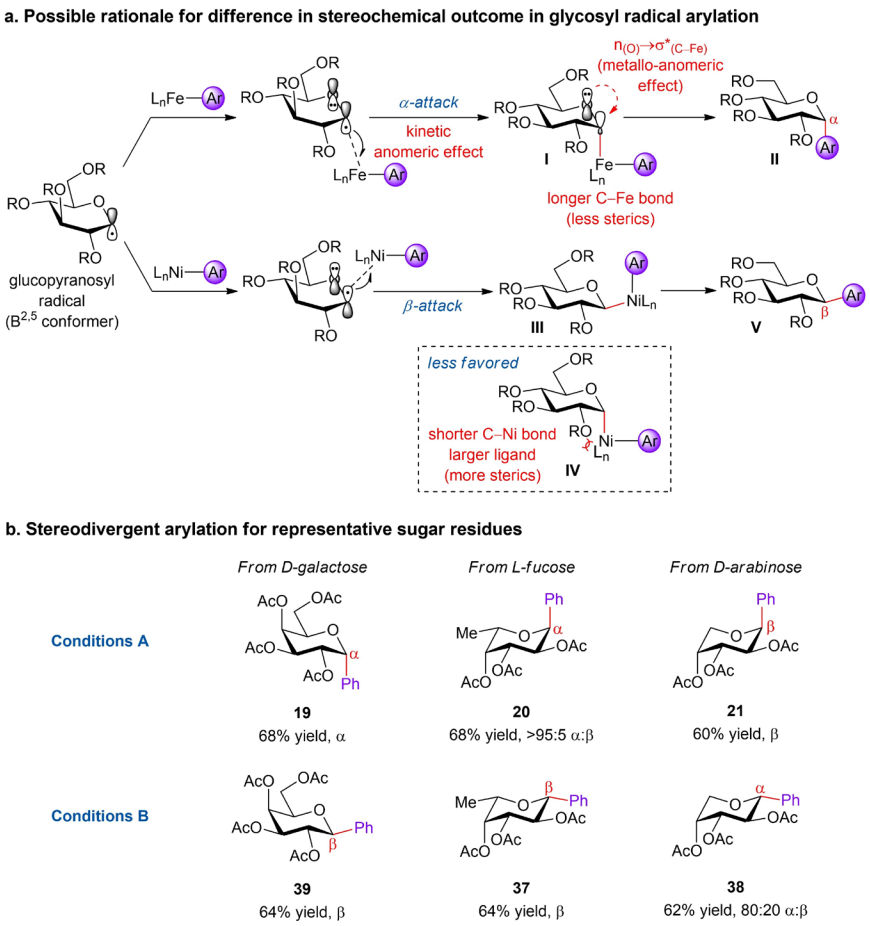

Scheme 4. Stereodivergent *C*-aryl glycosylation.

and steric effects reinforce each other (for example, **22**, **23**, **41**, **42** in Tables 1 and 2). In these cases, only a single diastereomer could be generated.

Control experiments were carried out to provide support for the intermediacy of radicals in the catalytic transformations (Scheme 5). Performing the standard Fe-catalyzed cross-coupling of 1 in the presence of exogenous TEMPO (1.5 equiv) drastically inhibited the reaction (25% conv., <2% 2), and 1 0% of the desulfonylated glycosyl-TEMPO adduct 45 was detected by GCMS analysis (Scheme 5a). This result suggests the in situ formation of a reactive glycosyl radical intermediate (via activation of 1 by a low-valent organoiron species[38,39] with concomitant formation of sulfinate[38,50]) which was captured by TEMPO in the reaction medium.

On the other hand, conducting the standard Ni-catalyzed cross-coupling of **3** in the presence of exogenous methyl acrylate (3 equiv) furnished the expected **4** in 37% yield and 20% of the glycosyl radical adduct **44**, in addition to 23% benzothiazole and 25% 2,2′-bibenzothiazole side products (generated in similar amounts vs. reaction without acrylate). Intriguingly, treatment of **3** with methyl acrylate and Zn in DMSO at 50 °C gave a mixture of **44**, **45** and **46**, suggesting that Zn was capable of reducing **3** to form glycosyl radical. The mode of sulfone activation likely arises from S–C(2-benzothiazoyl) bond cleavage[51–53] to generate 2-benzothiazoyl anion and a glycosylsulfonyl radical, which subsequently collapses to exude SO_2 and the glycosyl radical (see Scheme 6).

Based on insights gained from the present study as well as others,[35–38,53] proposed mechanisms for desulfonylative arylation under the two catalytic conditions are shown in Scheme 6. As shown in Scheme 6a, formation of a catalytically active low-valent aryl iron[38,39] species **i** could be initiated by reaction of $FeBr_2$ with the diaryl zinc reagent. **i** could serve as a reducing agent by triggering single-electron transfer (SET)[38] to the electrophilic 2-pyridyl sulfone, affording **ii** and a radical anion that undergoes direct S–C(glycosyl) bond cleavage and fragmentation to form glycosyl radical and sulfinate.[32,38] Diastereoselective recombination of the glycosyl radical with **ii** furnishes glycosyliron intermediate **iii**, which then reductively eliminates to furnish the desired *C*-aryl glycoside and **iv**. Transmetallation of **iv** with the diaryl zinc regenerates **i**.

Under reductive conditions in the presence of excess Zn, a putative tBu_3-terpy-ligated low-valent nickel[54] complex **v**

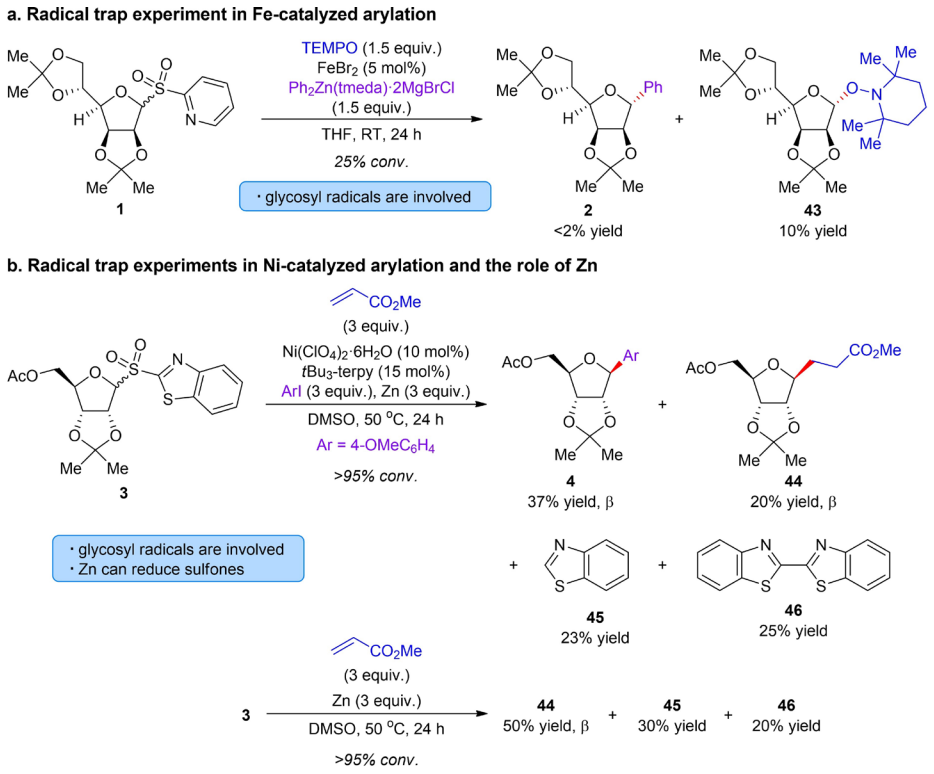

Scheme 5. Mechanistic studies. Conversions (conv.), yields and α:β ratios were determined by GC and GCMS analysis. See the Supporting Information for details.

is possibly generated, which undergoes oxidation addition with aryl iodide to give **vi** (Scheme 6b). Based on results in Scheme 5b, Zn is capable of reducing the more electrophilic 2-benzothiazolyl sulfone (via SET) to form a radical anion that undergoes S– C(2-benzothiazoyl) bond cleavage[51–53] to give glycosylsulfonyl radical and 2-benzothiazoyl anion. The glycosylsulfonyl radical readily undergoes desulfonylation by expelling SO_2 to afford glycosyl radical. An alternative pathway that cannot be completely ruled out is the in situ reduction of **vi** by Zn to afford a low-valent organonickel species, which may also activate the sulfone by SET.[53,55] Upon formation, the glycosyl radical associates with the Ni center in a diastereoselective manner to furnish **vii**. The ensuing reductive elimination delivers the desired *C*-aryl glycoside with concomitant generation of **viii**, which could be reduced by Zn to turn over the catalytic cycle.

Conclusion

In summary, we have shown that bench-stable heteroaryl glycosyl sulfones served as effective donors for C– C cross-coupling with aryl-substituted nucleophiles or electrophiles under Fe or Ni catalysis through distinct mechanisms. Isolable sulfones derived from a wide diversity of sugar residues, including typically unstable 2-deoxy and unprotected sugars, are amenable to the catalytic reactions to give the desired *C*-aryl glycosides with high stereochemical purity. For some classes of monosaccharides, stereodivergent access to both α and β isomers was possible. In light of their robustness and practicality, we expect the present transformations involving user-friendly glycosyl sulfones, soon to be commercially available, to find extensive utility in carbohydrate research for the preparation of complex glycan derivatives.

Acknowledgements

This research was supported by Research Scholarship Block from the Ministry of Education, Singapore: C-143-000-207-532, C-141-000-777-532, C-141-000-333-532 (M.J.K.). We thank Geok Kheng Tan for X-ray crystallographic analysis.

Conflict of Interest

The authors declare no conflict of interest.

Data Availability Statement

The data that support the findings of this study are available in the Supporting Information of this article.

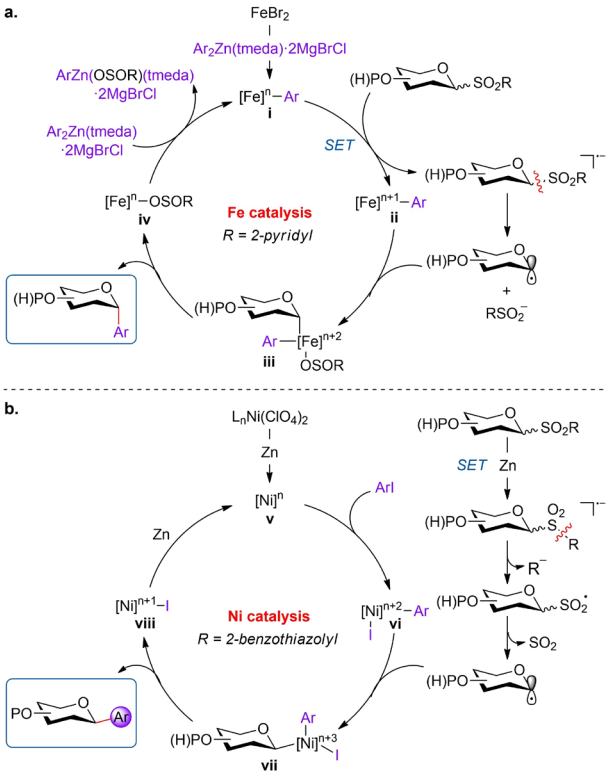

Scheme 6. Proposed mechanisms for Fe- and Ni-catalyzed C-aryl glycosylation.

Keywords: C-Aryl Glycosides · Cross-Coupling · Glycosyl Sulfones · Iron Catalysis · Nickel Catalysis

[1] L. Somsák, *Chem. Rev.* **2001**, *101*, 81–135.
[2] É. Bokor, S. Kun, D. Goyard, M. Tóth, J. Praly, S. Vidal, L. Somsák, *Chem. Rev.* **2017**, *117*, 1687–1764.
[3] Y. Yang, B. Yu, *Chem. Rev.* **2017**, *117*, 12281–12356.
[4] A. Dondoni, A. Marra, *Chem. Rev.* **2000**, *100*, 4395–4422.
[5] T. Bililign, B. R. Griffithbc, J. S. Thorson, *Nat. Prod. Rep.* **2005**, *22*, 742–760.
[6] J. Štambaský, M. Hocek, P. Kocovsky, *Chem. Rev.* **2009**, *109*, 6729–6764.
[7] S. Manabe, Y. Ito, *J. Am. Chem. Soc.* **1999**, *121*, 9754–9755.
[8] T. Nishikawa, Y. Koide, S. Kajii, K. Wada, M. Ishikawaa, M. Isobe, *Org. Biomol. Chem.* **2005**, *3*, 687–700.
[9] Q. Wang, Y. Fu, W. Zhu, S. An, Q. Zhou, S.-F. Zhu, G. He, P. Liu, G. Chen, *CCS Chem.* **2020**, *2*, 1729–1736.
[10] T. Nishikawa, M. Ishikawa, M. Isobe, *Synlett* **1999**, 123–125.
[11] Q. Wang, S. An, Z. Deng, W. Zhu, Z. Huang, G. He, G. Chen, *Nat. Catal.* **2019**, *2*, 793–800.
[12] E. C. Chao, R. R. Henry, *Nat. Rev. Drug Discovery* **2010**, *9*, 551–559.
[13] K. Krohn, A. Agocs, C. Bäuerlein, *J. Carbohydr. Chem.* **2003**, *22*, 579–592.
[14] H. Liao, J. Ma, H. Yao, X.-W. Liu, *Org. Biomol. Chem.* **2018**, *16*, 1791–1806.
[15] Z. Guo, J. Bai, M. Liu, D. Xiong, X. Ye, *Chin. J. Org. Chem.* **2020**, *40*, 3094–3111.
[16] L.-Y. Xu, N.-L. Fan, X.-G. Hu, *Org. Biomol. Chem.* **2020**, *18*, 5095–5109.
[17] A. Chen, L. Xu, Z. Zhou, S. Zhao, T. Yang, F. Zhu, *J. Carbohydr. Chem.* **2021**, *40*, 361–400.
[18] A. Chen, B. Yang, Z. Zhou, F. Zhu, *Chem. Catal.* **2022**, *2*, 3430–3470.
[19] Q. Wang, Q. Sun, Y. Jiang, H. Zhang, L. Yu, C. Tian, G. Chen, M. J. Koh, *Nat. Synth.* **2022**, *1*, 235–244.
[20] Y. Wei, Q. Wang, M. J. Koh, *Angew. Chem. Int. Ed.* **2022**, *61*, e202214247; *Angew. Chem.* **2022**, *134*, e202214247.
[21] Y. Wei, B. Ben-Zvi, T. Diao, *Angew. Chem. Int. Ed.* **2021**, *60*, 9433–9438; *Angew. Chem.* **2021**, *133*, 9519–9524.
[22] J. Liu, H. Gong, *Org. Lett.* **2018**, *20*, 7991–7995.
[23] A. Dumoulin, J. K. Matsui, Á. Gutiérrez-Bonet, G. A. Molander, *Angew. Chem. Int. Ed.* **2018**, *57*, 6614–6618; *Angew. Chem.* **2018**, *130*, 6724–6728.
[24] F. Zhu, M. J. Rourke, T. Yang, J. Rodriguez, M. A. Walczak, *J. Am. Chem. Soc.* **2016**, *138*, 12049–12052.
[25] F. Zhu, J. Rodriguez, S. O'Neill, M. A. Walczak, *ACS Cent. Sci.* **2018**, *4*, 1652–1662.
[26] F. Zhu, J. Rodriguez, T. Yang, I. Kevlishvili, E. Miller, D. Yi, S. O'Neill, M. J. Rourke, P. Liu, M. A. Walczak, *J. Am. Chem. Soc.* **2017**, *139*, 17908–17922.
[27] C. S. Bennett, M. C. Galan, *Chem. Rev.* **2018**, *118*, 7931–7985.
[28] S. Meng, X. Li, J. Zhu, *Tetrahedron* **2021**, *88*, 132140.
[29] J. Zeng, Y. Xu, H. Wang, L. Meng, Q. Wan, *Sci. China Chem.* **2017**, *60*, 1162–1179.
[30] K. Villadsen, M. C. Martos-Maldonado, K. J. Jensen, M. B. Thygesen, *ChemBioChem* **2017**, *18*, 574–612.
[31] N. Miquel, G. Doisneau, J.-M. Beau, *Angew. Chem. Int. Ed.* **2000**, *39*, 4111–4114; *Angew. Chem.* **2000**, *112*, 4277–4280.
[32] B. M. Trost, C. A. Kalnmals, *Chem. Eur. J.* **2019**, *25*, 11193–11213.
[33] N. Oka, A. Mori, K. Suzuki, K. Ando, *J. Org. Chem.* **2021**, *86*, 657–673.
[34] Q. Wang, B. C. Lee, T. J. Tan, Y. Jiang, W. H. Ser, M. J. Koh, *Nat. Synth.* **2022**, *1*, 967–974.
[35] M. Nambo, Y. Maekawa, C. M. Crudden, *ACS Catal.* **2022**, *12*, 3013–3032.
[36] J. Corpas, S.-H. Kim-Lee, P. Mauleón, R. G. Arrayás, J. C. Carretero, *Chem. Soc. Rev.* **2022**, *51*, 6774–6823.
[37] L. Gong, H.-B. Sun, L.-F. Deng, X. Zhang, J. Liu, S. Yang, D. Niu, *J. Am. Chem. Soc.* **2019**, *141*, 7680–7686.
[38] W. Miao, Y. Zhao, C. Ni, B. Gao, W. Zhang, J. Hu, *J. Am. Chem. Soc.* **2018**, *140*, 880–883.
[39] L. Adak, S. Kawamura, G. Toma, T. Takenaka, K. Isozaki, H. Takaya, A. Orita, H. C. Li, T. K. M. Shing, *J. Am. Chem. Soc.* **2017**, *139*, 10693–10701.
[40] S. Oae, T. Kawai, N. Furukawa, *Phosphorous and Sulfur* **1987**, *34*, 123–132.
[41] A. G. Draffan, et al., *ACS Med. Chem. Lett.* **2014**, *5*, 679–684.
[42] J. W. Scott, M. E. Rasche, *J. Bacteriol.* **2002**, *184*, 4442–4448.
[43] Y. Li, Z. Wang, L. Li, X. Tian, C. Li, *Angew. Chem. Int. Ed.* **2022**, *61*, e202110391; *Angew. Chem.* **2022**, *134*, e202110391.
[44] C. E. I. Knappke, S. Grupe, D. Gärtner, M. Corpet, C. Gosmini, A. J. von Wangelinet, *Chem. Eur. J.* **2014**, *20*, 6828–6842.
[45] B. Giese, *Angew. Chem. Int. Ed. Engl.* **1989**, *28*, 969–980; *Angew. Chem.* **1989**, *101*, 993–1004.
[46] F. Zhu, M. A. Walczak, *J. Am. Chem. Soc.* **2020**, *142*, 15127–15136.
[47] A. G. Orpen, L. Brammer, F. H. Allen, O. Kennard, D. G. Watson, R. Taylor, *J. Chem. Soc. Dalton Trans.* **1989**, S1–S83.
[48] J. Liu, C. Lei, H. Gong, *Sci. China Chem.* **2019**, *62*, 1492–1496.
[49] C. Zhang, S.-Y. Xu, H. Zuo, X. Zhang, Q.-D. Dang, D. Niu, *Nat. Synth.* **2023**, *2*, 251–260.
[50] S. E. Denmark, A. J. Cresswell, *J. Org. Chem.* **2013**, *78*, 12593–12628.

[51] Y. Chen, N. McNamara, O. May, T. Pillaiyar, D. Blakemore, S. V. Ley, *Org. Lett.* **2020**, *22*, 5746–5748.
[52] M. Nambo, Y. Tahara, J. C. Yim, D. Yokogawa, C. M. Crudden, *Chem. Sci.* **2021**, *12*, 4866–4871.
[53] J. M. E. Hughes, P. S. Fier, *Org. Lett.* **2019**, *21*, 5650–5654.
[54] J. Liu, Y. Ye, J. L. Sessler, H. Gong, *Acc. Chem. Res.* **2020**, *53*, 1833–1845.
[55] R. R. Merchant, J. T. Edwards, T. Qin, M. M. Kruszyk, C. Bi, G. Che, D. H. Bao, W. Qiao, L. Sun, M. R. Collins, O. O. Fadeyi, G. M. Gallego, J. J. Mousseau, P. Nuhant, P. S. Baran, *Science* **2018**, *360*, 75–80.
[56] Deposition numbers 2126411 (for **d-20**), 2170509 (for **SI-1**), 2169287 (for **35**) contain the supplementary crystallographic data for this paper. These data are provided free of charge by the joint Cambridge Crystallographic Data Centre and Fachinformationszentrum Karlsruhe Access Structures service.

Manuscript received: January 20, 2023
Accepted manuscript online: March 7, 2023
Version of record online: March 24, 2023

Chemistry–A European Journal
Research Article
doi.org/10.1002/chem.202201356
Chemistry Europe
European Chemical Societies Publishing

www.chemeurj.org

Copper-Catalyzed Carbonylative Cross-Coupling of Alkyl Iodides and Amines

Johanne Ling,[a] Antoine Bruneau-Voisine,[b] Guillaume Journot,[b] and Gwilherm Evano*[a]

Abstract: A general copper-catalyzed carbonylative cross-coupling between amines and alkyl iodides is reported. Using a simple combination of catalytic amounts of copper(I) chloride and *N,N,N′,N″,N″*-pentamethyldiethylenetriamine in the presence of sodium hydroxide under carbon monoxide pressure, a broad range of alkyl iodides and amines can be efficiently coupled to the corresponding amides that are obtained in good to excellent yields. Notable features of this process – the first one relying on a base metal catalyst – include the availability and low cost of the catalytic system, its successful use with primary, secondary, tertiary alkyl iodides and all classes of amines – with no or limited competing nucleophilic substitution without CO incorporation – as well as its efficiency with complex alkyl iodides and amines. Mechanistic studies demonstrated that a radical pathway is operative and the key role of CO.

Introduction

Amides are among the most prevalent building blocks in chemical synthesis and are found in a variety of natural products and bioactive molecules that had a deep impact on human health. The synthesis of amides is thus one of the most widespread processes not only in organic chemistry research laboratories but also from an industrial perspective, finding applications, for example, in the synthesis of bulk chemicals, polymers, agrochemicals or active pharmaceutical ingredients.

They are conveniently prepared from carboxylic acids and amines, a reaction that however requires the preactivation of the acid mediated by a stoichiometric activating agent, generating undesired waste and showing poor atom economy. As a consequence, and due to the importance of amide synthesis, a range of alternative strategies for amide bond formation have been investigated.[1] Among these, the three-component coupling between organic halides, amines and carbon monoxide is one of the most attractive options. Such carbonylative cross-coupling reactions have been extensively developed for the synthesis of benzamides from aryl halides, following pioneering studies reported by Heck in 1974 using palladium catalysis,[2] and various non-noble metal-based catalysts have been shown over the years to efficiently catalyze such processes (Figure 1a).[3] In sharp contrast, they are still underdeveloped in the alkyl series, notably due to competing direct nucleophilic substitution without CO incorporation, β-hydride elimination or metal migration in alkyl-metal complexes, as well as double insertion of carbon monoxide.[4] CO being moreover a strong π-acidic ligand, it typically hampers the oxidative addition of the metal complexes onto the C(sp^3)-X bond.

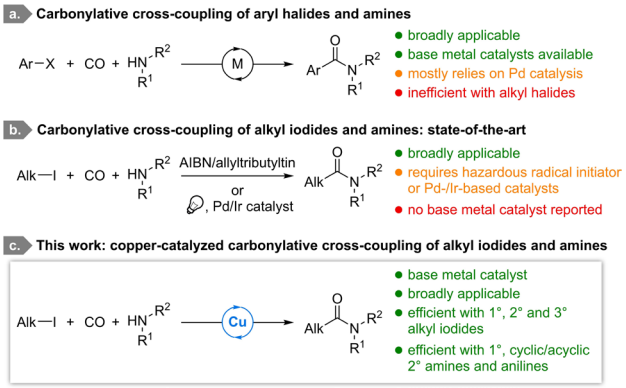

Figure 1. Carbonylative cross-coupling of organic halides and amines: state-of-the-art and current work.

While the feasibility of radical carbonylative cross-coupling reactions between amines and alkyl iodides has however been demonstrated, with pioneering studies from the Ryu group,[5] they require either the use of toxic and hazardous radical initiators[5] or a palladium-/iridium- based catalyst in the presence of a light source (Figure 1b),[6] major limitations still remain in terms of applicability and cost-efficiency. Despite a gain in interest in recent years due to the higher natural abondance and generally lower toxicity of first row transition metal complexes,[7] there is a strong need for alternative processes based on base metal catalysts associated with simple ligands,[8] which remain untapped for this application. Meeting this challenge would be of high significance in the many areas

[a] *Dr. J. Ling, Prof. G. Evano*
Laboratoire de Chimie Organique, Service de Chimie et Physico-Chimie Organiques
Université libre de Bruxelles (ULB)
Avenue F.D. Roosevelt 50, CP160/06, 1050 Brussels (Belgium)
E-mail: Gwilherm.Evano@ulb.be

[b] *Dr. A. Bruneau-Voisine, Dr. G. Journot*
Oril Industrie
13, rue Auguste Desgenétais, CS 60125, 76210 Bolbec (France)

Supporting information for this article is available on the WWW under https://doi.org/10.1002/chem.202201356

Chemistry–A European Journal
Research Article
doi.org/10.1002/chem.202201356
Chemistry Europe
European Chemical Societies Publishing

in which amides are commonly utilized. Based on our long-standing interest in copper-catalyzed cross-coupling[9] and radical[10] reactions, and inspired by the seminal work of the Mankad[11] group on the copper-catalyzed aminocarbonylation of alkyl iodides with nitroarenes and related alkoxycarbonylation reactions,[12] we envisioned that the proper combination of a copper(I) source and a ligand – which has to form a complex stable enough to avoid its displacement with excess carbon monoxide – facilitating the single electron activation of the starting alkyl iodide could promote the carbonylative cross-coupling between amines and alkyl iodides (Figure 1c).[13,14] We report in this manuscript the development of such a process and its broad applicability, notably with complex substrates.[15]

Results and Discussion

Based on this working hypothesis, we initiated our studies by a systematic screening of the influence of the different reaction parameters using iodocyclohexane **1a** and morpholine **2a** as model substrates. First trials gratifyingly led to the formation of the desired amide **3a** and revealed the superiority of copper(I) chloride as the copper source, sodium hydroxide as the base, in 1,4-dioxane or THF at 0.1 M, the crude reaction mixture being cleaner in the former, for 15 h at 70 °C and under a 5 bar pressure of carbon monoxide (see Supporting Information, Tables S1–S4). As a note, the reaction still proceeds with a reduced pressure of carbon monoxide, but with a diminished efficiency (66% NMR yield - see Supporting Information, Table S4), which might be however interesting for some applications. In this perspective, solid sources of carbon monoxide ($Mo(CO)_6$, $W(CO)_6$ and $Co_2(CO)_8$) were also evaluated but the carbonylated product **3a** was not observed under these conditions. Notably, the choice of sodium hydroxide was crucial for the reaction to efficiently proceed and an excess of this base is required for the reaction to efficiently proceed, certainly due to its limited solubility in 1,4-dioxane. The influence of the ligand on the carbonylative cross-coupling reaction was next evaluated using a series of representative ligands for copper including NHCs, bipyridine and polyamines, most of these ligands being known to facilitate copper-catalyzed atom transfer radical polymerization (ATRP)[16] and cyclization (ATRC)[17] reactions. Results from this study are shown in Figure 2.

Interestingly, apart from IMes NHC precursor 1,3-bis(2,4,6-trimethylphenyl)imidazoliumchloride L_1, all the ligands we tested afforded the carbonylated cross-coupling product **3a** in yields higher than 70% (Figure 2). The carbonylative coupling can indeed be promoted by NHCs (L_2, L_3), bipyridine (L_4) as well as bidentate (L_9–L_{11}), tridentate (L_6) and tetradentate (L_5, L_7, L_8) polyamines. Even if 1,3-bis(*iso*propyl)imidazolium chloride L_3 led to the best result (96% NMR yield), PMDETA L_6, which displayed similar performances (93% NMR yield) while being significantly cheaper, was selected as the ligand of choice since it offers the best compromise between performance, availability, and cost. Control experiments revealed that the presence of copper(I) chloride and the base were essential for the reaction to proceed while in the absence of ligand, the carbonylative coupling was

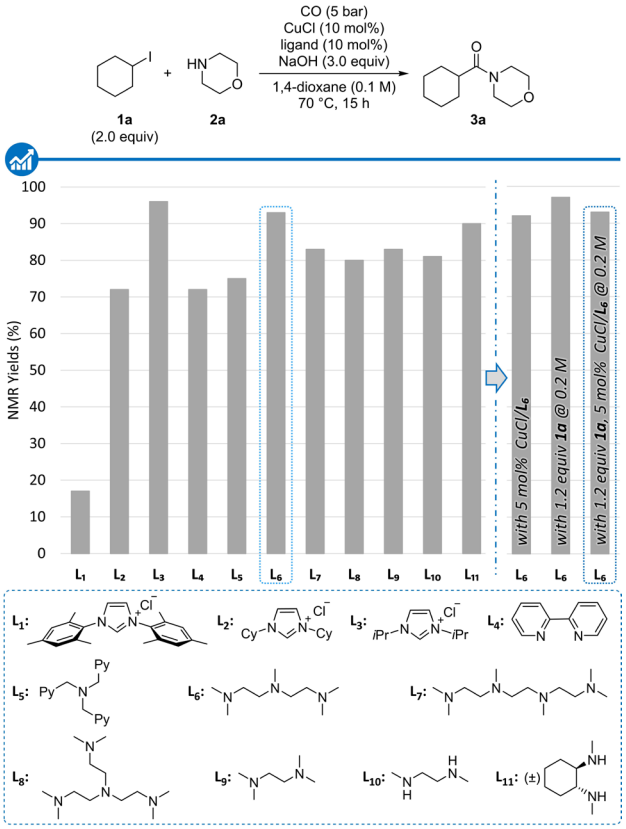

Figure 2. Validation of the working hypothesis and ligand screening. NMR yields determined by ^{1}H NMR analysis of crude reaction mixtures using 1,1,2,2-tetrachloroethane as internal standard. Py: 2-pyridyl.

still operative, despite a reduced efficiency, the starting amine and/or carbon monoxide acting both as (a) ligand(s) and reactant(s) in this case. Importantly, potential contamination with traces of palladium was ruled out since a similar efficiency was obtained with ultra-high purity reactants and solvents.

In an effort to further optimize the reaction conditions, the catalytic loading could be reduced to 5 mol% of both CuCl and PMDETA without affecting the yield and the excess of cyclohexyl iodide could be reduced to 1.2 equivalents with similar efficiency, amide **3a** being obtained in 93% NMR yield and 91% isolated yield (Figure 2).

With these optimized conditions in hands, we then moved to the study of the scope and limitations of this carbonylative cross-coupling reaction, first focusing on the influence of the starting alkyl iodide **1**, using morpholine **2a** as the model amine. Results from this study, shown in Figure 3, reveal the generality and rather broad scope of this copper-catalyzed aminocarbonylation. Secondary alkyl iodides were indeed readily transformed to the corresponding amides **3a**–**h** in good to excellent yields, except in the case of 4-iodotetrahydro-2*H*-pyran which failed to undergo the cross-coupling to **3i**. The reaction was moreover found to be highly diastereoselective when starting from an iodide derived from (−)-menthol, **3d** being obtained as a single diastereoisomer, and no products

Chemistry–A European Journal
Research Article
doi.org/10.1002/chem.202201356
Chemistry Europe
European Chemical Societies Publishing

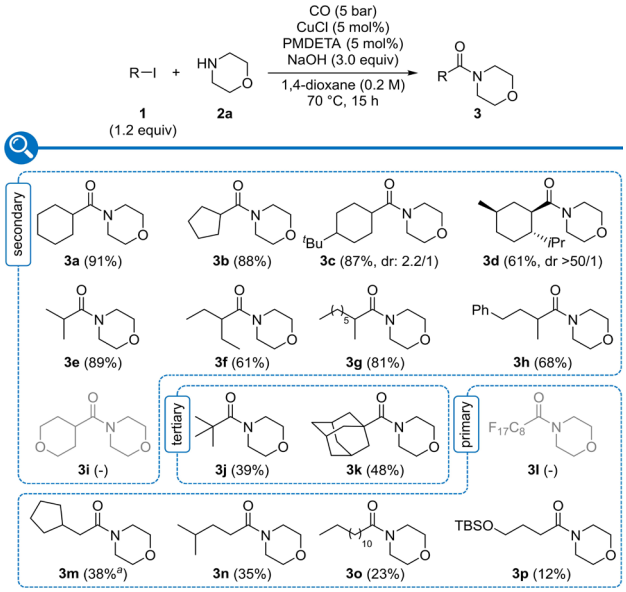

Figure 3. Scope of the copper-catalyzed aminocarbonylation with representative alkyl iodides. [a] At 0.1 M.

resulting either from direct nucleophilic substitution or double insertion of carbon monoxide could be detected in crude reaction mixtures. To our delight, even challenging tertiary alkyl iodides were found to be suitable reaction partners, although with reduced efficiency, as illustrated with the synthesis of **3j** and **3k** that could be obtained in 39% and 48% yields, respectively. As for primary alkyl iodides, although they still afforded the corresponding amides **3m–p**, their carbonylative cross-coupling was more sluggish and the yields were found to be in the lower range. In the case of highly reactive perfluorooctyl iodide, the competing direct nucleophilic substitution could not be suppressed and amide **3l** was thus not obtained. As a note, cyclohexyl bromide was found to be unreactive under the reaction conditions, which is in line with its more challenging activation by both single or two electron processes, and an attempt to perform an in situ retro-Finkelstein reaction with additional sodium iodide failed.

We next moved to the study of the influence of the amine on the copper-catalyzed aminocarbonylation, using this time iodocyclohexane **1a** as the reference alkyl electrophile. As highlighted by results collected in Figure 4, a broad range of primary and secondary amines, including cyclic and acyclic ones, could be efficiently utilized, the corresponding amides **3a**, **3q–3ar** being obtained in good to excellent yields in most cases. Sterically hindered amines such as *tert*-butylamine or

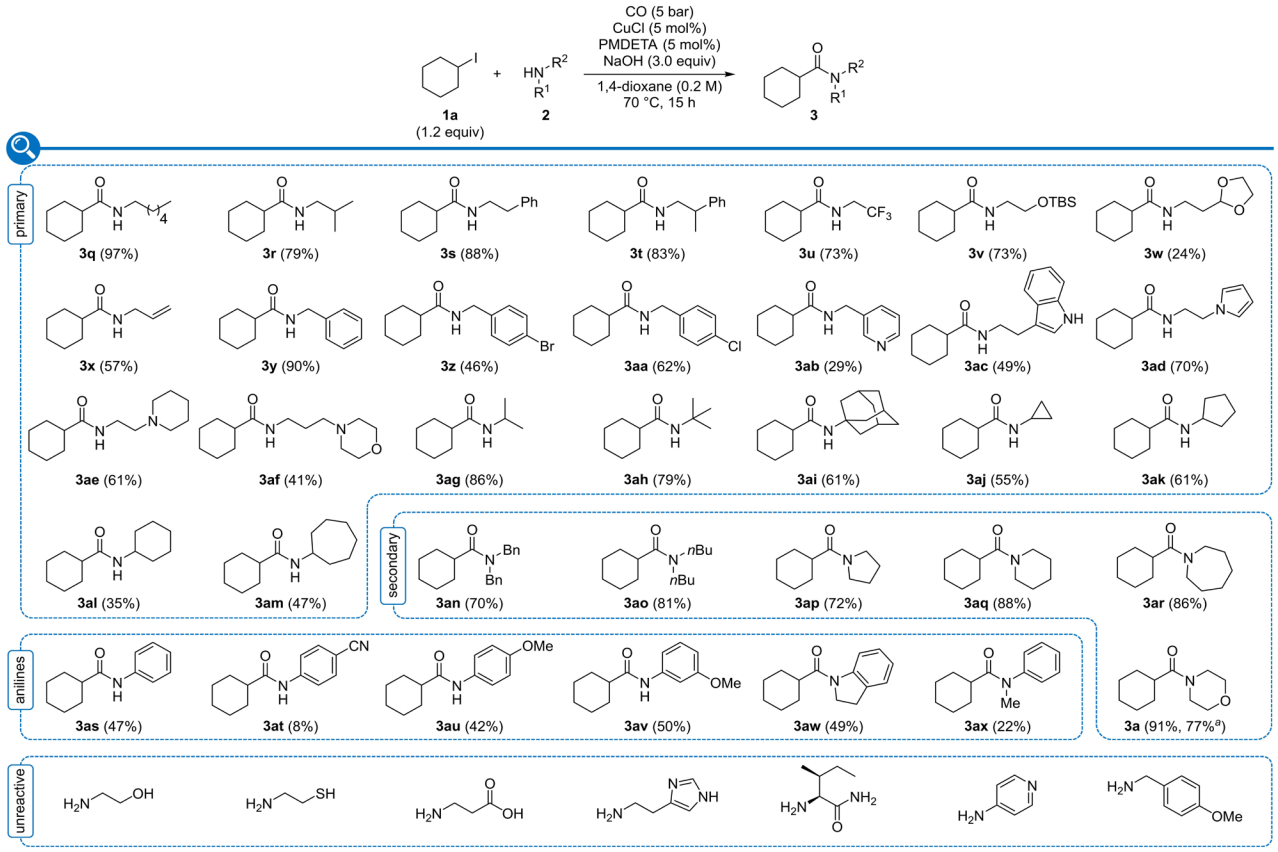

Figure 4. Scope of the copper-catalyzed aminocarbonylation with representative amines. [a] Reaction performed on a 3 gram scale.

Chemistry–A European Journal
Research Article
doi.org/10.1002/chem.202201356
Chemistry Europe
European Chemical Societies Publishing

adamanty lamine were shown to be suitable reaction partners, the corresponding amides **3 ah** and **3 ai** being obtained in 79 % and 61 % y ields, respectively . Even a poorly nucleophilic amine such as 2,2,2-trifluoroethy lamine was readily transformed, amide **3 u** being isolated in 73 % y ield, and a range of functional groups including ary l groups (**3 s**,**t**,**y**,**z**,**aa**), an alkene (**3 x**), a cy clopropane (**3 aj**), a sily l ether (**3 v**), and a ketal (**3 w**) were tolerated, the last one however giving a lower y ield most certainly due to partial hy droly sisHeteroarenes such as a py ridine (**3 ab**), an indole (**3 ac**) or a py rrole (**3 ad**) were shown to be compatible with our reaction conditions, the former y ielding to a much lower y ield however, which can be attributed to a competing coordination to the copper-based cataly st, and the presence of heterocy clic sy stems on the starting amine such as a piperidine (**3 ae**) or a morpholine (**3 af**) was also tolerated. Importantly, an aryl bromide (**3 z**) or chloride (**3 aa**) was not activated, which provides interesting opportunities for post-functionalization and diversification. Primary and secondary amines performed equally well and competing dehy drogenation of the starting amines was never observed.[18] Importantly , the aminocarbony lation could be extended to less nucleophilic anilines, however with a more pronounced impact on the reactivity and a greater substrate-dependence. Indeed, while aniline and electron-rich anisidines were aminocarbonylated to the corresponding amides **3 as**, **3 au** and **3 av** in fair y ields, the use of an electron-poor aniline such as *p*-cyanoaniline or *N*-methy l-aniline resulted in lower y ields of 8 % (**3 at**) and 22 % (**3 ax**), respectively . In addition to chelating amines such as aminoethanol, cy steamine, β-alanine, histamine, isoleucinamide or 4-aminopy ridine, which could definitely poison the copper-based catalyst, this represents the main limitation of our copper-cataly zed carbony lative cross-coupling with respect to the amines that can be utilized. Importantly , the reaction is not limited to the small scale used for the scope and limitation studies since the copper-cataly zed coupling of **1 a**, **2 a** and CO could be efficiently performed on a 3 gram scale, amide **3 a** being isolated in 77 % y ield, in a virtually pure form, upon simple filtration and concentration under reduced pressure.

In an attempt to push further the limits of our copper-cataly zed carbony lative cross-coupling of alky l iodides and amines and evaluate its efficiency in "real life" situations, the reaction with complex amines or iodides was next envisioned. As highlighted in Scheme 1, L-proline ester **2 b** could be successfully coupled with cy clohexy l iodide **1 a** under our standard conditions to afford amide **3 ay** in 67 % y ield and with only a slight erosion of the optical purity , even when the reaction time was extended to 3 days. An even higher efficiency was obtained for the carbony lative coupling of *N*-aryl-piperazine **2 c**, the corresponding amide **3 az** being obtained in 87 % y ield, here again without competing direct nucleophilic substitution or double insertion of carbon monoxide. The reaction is moreover amenable to the carbony lation of natural product or natural product-derived amines or iodides, as illustrated with the sy nthesis of abiety lamine- or estradiol- derived amides **3 ba** and **3 bb**, complex amides that could be obtained in 73 % and 33 % y ields, respectively , the lower y ield obtained for the latter being certainly due to the limited stability of **1 b** and the

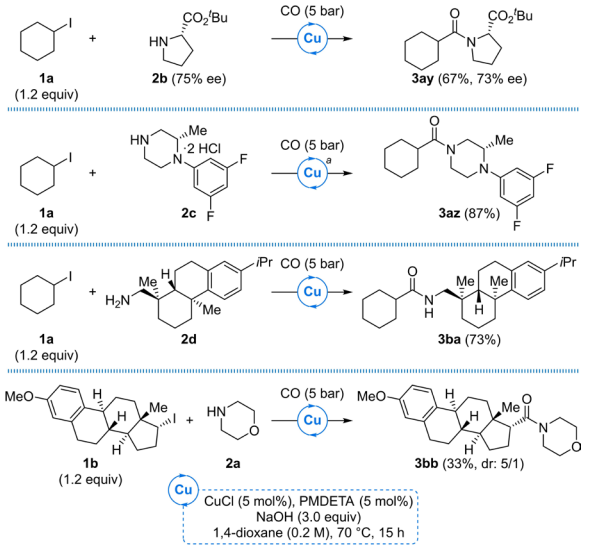

Scheme 1. Scope of the copper-catalyzed aminocarbonylation with complex substrates. [a] With 5 equivalents of sodium hydroxide.

diastereoselectivity arising from preferential aminocarbonylation on the least hindered face.

After carefully studying the scope and limitations of this aminocarbonylation reaction, we then attempted to gain some insights into the reaction mechanism, a radical process being *a priori* operative. The implication of a radical pathway could indeed be unambiguously demonstrated with both the ring-opening observed starting with cyclopropylmethyl iodide **1 c** yielding unsaturated amide **3 bc** and the complete inhibition of the reaction in the presence of TEMPO (Scheme 2).

These experiments are clearly in line with a radical pathway. Combined with the reactivity of primary/secondary alkyl iodides that are in agreement with the relative stabilities of the corresponding radical species, the known difficult oxidative addition into C(sp^3)-X bonds, and the limited impact of the steric hindrance of the starting amine, the catalytic cycle shown in Figure 5 is most likely involved. It would be initiated by a single electron transfer from a copper(I) complex to the starting

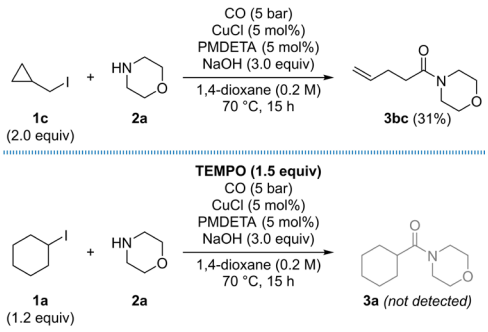

Scheme 2. Probing a radical pathway for the copper-catalyzed carbonylative cross-coupling of alkyl iodides and amines.

Chemistry–A European Journal
Research Article
doi.org/10.1002/chem.202201356
Chemistry Europe
European Chemical Societies Publishing

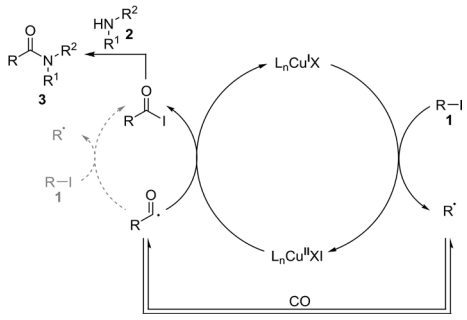

Figure 5. Possible catalytic cycle for the copper-catalyzed carbonylative cross-coupling of alkyl iodides and amines.

alkyl halide **1** generating the corresponding copper(II) complex and the alkyl radical species. Addition of the latter to carbon monoxide[19] would yield a transient acyl radical intermediate that would be next oxidized by the copper(II) complex, closing the catalytic cycle and yielding an intermediate acyl iodide. Its final reaction with the starting amine **2** in the presence of the base, required to trap the equivalent of hydriodic acid released, would then afford the desired carbonylated product **3**, this last step involving a highly reactive acyl iodide providing a rationale for the little difference observed in reactivity with sterically hindered amines. Importantly, the intermediacy of this acyl iodide is supported by the reaction of cyclohexanecarbonyl iodide with morpholine and aniline under our reaction conditions, affording the corresponding amides **3a** and **3as** in 59% and 48% yield, respectively, without detectable amounts of cyclohexanecarboxylic acid that would result from a competing reaction with sodium hydroxide (see Supporting Information for details). These results, which support our overall mechanism, are in line with the higher nucleophilicity of morpholine and aniline compared to the hydroxide anion ($N_{morpholine}$: 15.6[20] and $N_{aniline}$: 12.6–13.0[20b] vs. N_{OH^-}: 10.5[21] in the Mayr reactivity scale).[22] As a note, a radical chain pathway cannot be excluded, and the copper(I) complex would in this case act as a smart initiator. Importantly, while Cu^{I}(PMDETA) is a common catalyst for ATRP and ATRC,[16,17] it cannot be the actual catalytic species in this transformation due to its redox potentials being in disagreement with its ability to reduce unactivated alkyl halides.[23] Carbon monoxide might therefore have a dual role in this copper-catalyzed carbonylative cross-coupling reaction, acting not only as a C1 source but also as a key ligand that would facilitate the overall process, CO being known to have a strong impact on Cu(I)/Cu(II) redox potentials.[24]

Conclusion

In conclusion, we have reported an efficient and broadly applicable copper-catalyzed carbonylative cross-coupling of unactivated alkyl iodides and amines. Primary, secondary, and tertiary alkyl iodides and primary, cyclic, and acyclic secondary amines as well as anilines were all shown to be suitable reaction partners, affording the corresponding amides in good to excellent yields. A broad range of functional groups were found to be tolerated and the aminocarbonylation of both complex and highly functionalized alkyl iodides further highlights the efficiency of this three-component cross-coupling. In addition to being the first broadly applicable catalytic system for such an aminocarbonylation relying on a base metal, which should have an impact on amide synthesis, notable features include the availability and low cost of the metal source, the ligand as well as the base. Further studies to expand the scope of such carbonylative cross-coupling reactions are underway, notably to elucidate the key role of CO, and will be reported in due course.

Acknowledgements

This work was financially supported by Oril Industrie, affiliated to Les Laboratoires Servier, the Université libre de Bruxelles (ULB) and the FNRS (PDR T.0160.18). The authors gratefully thank Dr. Alexandre Le Flohic, Dr. Rodolphe Tamion, and Dr. Jean Fournier (Oril Industrie) for fruitful discussions as well as Dr. Lucile Vaysse-Ludot (Oril Industrie) for constant support. We are indebted to Ms. Omaïma Adaoudi and Mr. Yohann Landrain (ULB) for their valuable assistance during the revision of this manuscript as well as Dr. Cécile Verrier and Mrs. Perrine Maitrejean (Oril) for their help with HRMS analyses.

Conflict of Interest

The authors declare no conflict of interest.

Data Availability Statement

The data that support the findings of this study are available in the supplementary material of this article.

Keywords: amides · carbon monoxide · carbonylation · copper catalysis · cross-coupling

[1] For selected review articles, see: a) R. M. de Figueiredo, J.-S. Suppo, J.-M. Campagne, *Chem. Rev.* **2016**, *116*, 12029–12122; b) M. T. Sabatini, L. T. Boulton, H. F. Sneddon, T. D. Sheppard, *Nat. Catal.* **2019**, *2*, 10–17; c) A. S. Santos, A. M. S. Silva, M. M. B. Marques, *Eur. J. Org. Chem.* **2020**, *17*, 2501–2516.
[2] A. Schoenberg, R. F. Heck, *J. Org. Chem.* **1974**, *39*, 3327–3331.
[3] For representative examples, see: a) P. Giannoccaro, E. Pannacciulli, *J. Organomet. Chem.* **1987**, *317*, 119–127; b) A. M. Veatch, E. J. Alexanian, *Chem. Sci.* **2020**, *11*, 7210–7213.
[4] L. Wu, X. Fang, Q. Liu, R. Jackstell, M. Beller, X.-F. Wu, *ACS Catal.* **2014**, *4*, 2977–2989.
[5] I. Ryu, K. Nagahara, N. Kambe, N. Sonoda, S. Kreimerman, M. Komatsu, *Chem. Commun.* **1998**, 1953–1954.
[6] a) T. Fukuyama, S. Nishitani, T. Inouye, K. Morimoto, I. Ryu, *Org. Lett.* **2006**, *8*, 1383–1386; b) A. Fusano, S. Sumino, S. Nishitani, T. Inouye, K. Morimoto, T. Fukuyama, I. Ryu, *Chem. Eur. J.* **2012**, *18*, 9415–9422; c) S. Sumino, A. Fusano, T. Fukuyama, I. Ryu, *Acc. Chem. Res.* **2014**, *47*, 1563–1574; d) S. Y. Chow, M. Y. Stevens, L. Åkerbladh, S. Bergman, L. R. Odell, *Chem. Eur. J.* **2016**, *22*, 9155–9161; e) M. Sardana, J. Bergman, C. Ericsson, L. P. Kingston, M. Schou, C. Dugave, D. Audisio, C. S. Elmore, *J.*

Chemistry–A European Journal
Research Article
doi.org/10.1002/chem.202201356
Chemistry Europe
European Chemical Societies Publishing

Org. Chem. **2019**, *84*, 16076–16085; f) J. A. Forni, N. Micic, T. U. Connell, G. Weragoda, A. Polyzos, *Angew. Chem. Int. Ed.* **2020**, *59*, 18646–18654; *Angew. Chem.* **2020**, *132*, 18805–18813; g) G. M. Torres, Y. Liu, B. A. Arndtsen, *Science* **2020**, *368*, 318–323.

[7] a) K. S. Egorova, V. P. Ananikov, *Angew. Chem. Int. Ed.* **2016**, *55*, 12150–12162; *Angew. Chem.* **2016**, *128*, 12334–12347; b) K. H. Wedepohl, *Geochim. Cosmochim. Acta* **1995**, *59*, 1217–1232.

[8] For recent accounts, see: a) S. Shekhar, T. S. Ahmed, A. R. Ickes, M. C. Haibach, *Org. Process Res. Dev.* **2022**, *26*, 14–42; b) *Non-Noble Metal Catalysis: Molecular Approaches and Reactions* (Eds.: R. J. M. Klein Gebbink, M.-E. Moret), Wiley-VCH, Weinheim, **2018**.

[9] For selected recent contributions from our group on copper-catalyzed reactions, see: a) P. Thilmany, P. Gérard, A. Vanoost, C. Deldaele, L. Petit, G. Evano, *J. Org. Chem.* **2019**, *84*, 392–400; b) A. Nitelet, V. Kairouz, H. Lebel, A. B. Charette, G. Evano, *Synthesis* **2019**, *51*, 251–257; c) A. Nitelet, P. Gérard, J. Bouche, G. Evano, *Org. Lett.* **2019**, *21*, 4318–4321; d) S. Biswas, B. F. Van Steijvoort, M. Waeterschoot, N. R. Bheemireddy, G. Evano, B. U. W. Maes, *Angew. Chem. Int. Ed.* **2021**, *60*, 21988–21996; *Angew. Chem.* **2021**, *133*, 22159–22167.

[10] For representative contributions from our groups on copper-catalyzed radical reactions, see: a) C. S. Demmer, E. Benoit, G. Evano, *Org. Lett.* **2016**, *18*, 1438–1441; b) B. Michelet, C. Deldaele, S. Kajouj, C. Moucheron, G. Evano, *Org. Lett.* **2017**, *19*, 3576–3579; c) C. Theunissen, J. Wang, G. Evano, *Chem. Sci.* **2017**, *8*, 3465–3470; d) A. Nitelet, D. Thevenet, B. Schiavi, C. Hardouin, J. Fournier, R. Tamion, X. Pannecoucke, P. Jubault, T. Poisson, *Chem. Eur. J.* **2019**, *25*, 3262–3266; e) H. Baguia, G. Evano, *Chem. Eur. J.* **2022**, *28*, e202103599; f) C. Jacob, H. Baguia, A. Dubart, S. Oger, P. Thilmany, J. Beaudelot, C. Deldaele, S. Peruško, Y. Landrain, B. Michelet, S. Neale, E. Romero, C. Moucheron, V. Van Speybroeck, C. Theunissen, G. Evano, *Nat. Commun.* **2022**, *13*, 560.

[11] S. Zhao, N. P. Mankad, *Org. Lett.* **2019**, *21*, 10106–10110.

[12] a) Y. Li, X.-F. Wu, *Commun. Chem.* **2018**, *1*, 39; b) Y. Chen, L. Su, H. Gong, *Org. Lett.* **2019**, *21*, 4689–4693; c) H.-Q. Geng, X.-F. Wu, *Org. Lett.* **2021**, *23*, 8062–8066.

[13] For a review on copper-catalyzed cross-coupling reactions with unactivated alkyl electrophiles, see: L.-J. Cheng, N. P. Mankad, *Chem. Soc. Rev.* **2020**, *49*, 8036–8064.

[14] For a recent account on copper-catalyzed carbonylative coupling reactions with alkyl halides, see: L.-J. Cheng, N. P. Mankad, *Acc. Chem. Res.* **2021**, *54*, 2261–2274.

[15] After the submission of this manuscript, a related copper-catalyzed carbonylative cross-coupling of alkyl halides and amines has been reported by the Wu group: F. Zhao, H.-J. Ai, X.-F. Wu, *Angew. Chem. Int. Ed.* **2022**, *61*, e202200062; *Angew. Chem.* **2022**, *134*, e202200062.

[16] C. Boyer, N. A. Corrigan, K. Jung, D. Nguyen, T.-K. Nguyen, N. N. M. Adnan, S. Oliver, S. Shanmugam, J. Yeow, *Chem. Rev.* **2016**, *116*, 1803–1949.

[17] A. J. Clark, *Eur. J. Org. Chem.* **2016**, 2231–2243.

[18] For examples, see: a) R. D. Patil, S. Adimurthy, *Adv. Synth. Catal.* **2011**, *353*, 1695–1700; b) P. D. Sarmiento-Pavía, M. Flores-Álamo, A. Solano-Peralta, P. M. H. Kroneck, M. E. Sosa-Torres, *Inorg. Chim. Acta* **2018**, *481*, 189–196.

[19] C. Chatgilialoglu, D. Crich, M. Komatsu, I. Ryu, *Chem. Rev.* **1999**, *99*, 1991–2070.

[20] a) T. Kanzian, T. A. Nigst, A. Maier, S. Pichl, H. Mayr, *Eur. J. Org. Chem.* **2009**, 6379–6385; b) F. Brotzel, Y. Cheung Chu, H. Mayr, *J. Org. Chem.* **2007**, *72*, 3679–3688.

[21] S. Minegishi, H. Mayr, *J. Am. Chem. Soc.* **2003**, *125*, 286–295.

[22] In the case of a less nucleophilic amine such as 4-cyano-aniline, which did only give the corresponding amide **3at** in 8% yield (Figure 4), its reaction with cyclohexanecarbonyl iodide under our optimized reaction conditions did only produce the corresponding amide in 61% yield, without a trace of cyclohexanecarboxylic acid. The lower yield obtained for the carbonylative cross coupling of 4-cyano-aniline might thus be a result of both its reduced nucleophilicity and side reactions involving the addition of radical species to this electron-poor aniline.

[23] J. Qiu, K. Matyjaszewski, L. Thouin, C. Amatore, *Macromol. Chem. Phys.* **2000**, *201*, 1625–1631.

[24] a) P. Zanello, P. Leoni, *Can. J. Chem.* **1985**, *63*, 922–927; b) R. M. Hernandez, L. Aiken, P. K. Baker, M. Kalaji, *J. Electroanal. Chem.* **2002**, *520*, 53–63; c) H. C. Fry, H. R. Lucas, A. A. Narducci Sarjeant, K. D. Karlin, G. J. Meyer, *Inorg. Chem.* **2008**, *47*, 241–256.

Manuscript received: May 3, 2022
Accepted manuscript online: May 25, 2022
Version of record online: June 17, 2022

Nickel Catalysis

Reactivity in Nickel-Catalyzed Multi-component Sequential Reductive Cross-Coupling Reactions

Haifeng Chen, Huifeng Yue, Chen Zhu, and Magnus Rueping**

Abstract: The nickel-catalyzed three-component reductive carbonylation of alkyl halides, aryl halides, and ethyl chloroformate is described. Ethyl chloroformate is utilized as a safe and readily available source of CO in this multi-component protocol, providing an efficient and practical alternative for the synthesis of aryl-alkyl ketones. The reaction exhibits a wide substrate scope and good functional group compatibility. Experimental and DFT mechanistic studies highlight the complexity of the cross-electrophile coupling and provide insight into the sequence of the three consecutive oxidative additions of aryl halide, chloroformate, and alkyl halide.

Introduction

Reductive cross-electrophile coupling reactions have emerged as powerful and effective strategies in the construction of organic molecules. In these reactions, two electrophiles, often aryl- and alkyl halides, are employed with the challenge of suppressing unwanted homocouplings, and to achieve the selective cross electrophile C–C bond formation.[1] The mechanistic pathways (i.e., "radical-chain" and "sequential-reduction") are determined by the activation sequence of the electrophiles. An in-depth understanding of these reaction mechanisms is important for future catalyst design, improved selectivity and targeted application. However, the diversity of reaction mechanisms and the presence of nickel intermediates with multiple valence states make such studies rather challenging.[2] Recent reports suggest that the Ni^{I}-intermediate is the initial active catalytic species (Figure 1a).[3–5] Further detailed mechanistic investigations by Diao describe the chemoselectivity in cross-electrophile couplings. These studies shed light on the activation sequence and selectivity of two electrophiles, namely the C_{sp2} and C_{sp3} electrophiles that are activated by Ni^{I}-Br and Ni^{I}-Ar species, respectively (Figure 1a).[3a] In addition, Hu and co-workers described a reductive cross-coupling of alkyl halides and chloroformate via the initial formation of a Ni^{0} complex and oxidative addition to chloroformate to generate a Ni^{II}-species (Figure 1b).[6] Based on our research in the field of reductive cross-coupling reactions and inspired by the pioneering work[6,7] we became interested in multi-component cross-electrophile couplings as such transformations constitute several challenges, including the inherent complexity, the reactivity of the electrophiles, the sequence of oxidative additions and the control and understanding of chemoselectivity and product formation (Figure 1c).

To the best of our knowledge, a reductive, multi-component, cross-electrophile coupling for the formation of aryl-alkyl ketones has not been reported, which may be due to the complexity, selectivity, and the possible generation of several by-products (Figure 1c). Ketones are one of the most prevalent structural motifs found in bioactive natural

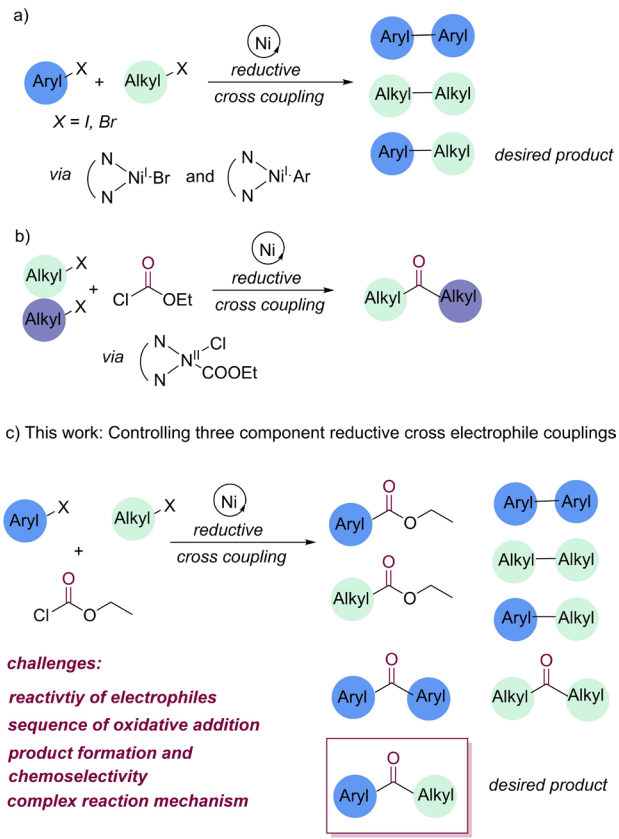

Figure 1. Development of a new catalytic carbonylation via nickel-catalyzed three-component cross-electrophile coupling.

[*] Dr. H. Chen, Dr. H. Yue, Dr. C. Zhu, Prof. Dr. M. Rueping
KAUST Catalysis Center (KCC), King Abdullah University of Science and Technology (KAUST)
Thuwal 23955-6900 (Saudi Arabia)
E-mail: chen.zhu@kaust.edu.sa
magnus.rueping@kaust.edu.sa

products, pharmaceuticals, materials, and biofuels.[8] Conventional approaches to access such compounds rely on transition-metal catalyzed carbonylation reactions. The use of air-sensitive organometallic reagents together with carbonyl precursors such as CO gas or metal carbonyl complexes may limit their application.[9–11] Nickel catalyzed two-component reductive cross-couplings of carboxylic acid derivatives provide good alternatives.[12] Herein, we report the nickel-catalyzed three-component reductive cross-coupling of alkyl halides, aryl iodide, and ethyl chloroformate. The protocol is notable for its simplicity, safety, broad substrate scope, and control of the consecutive activation of three different electrophiles.

Results and Discussion

Based on the reactivity and chemoselectivity challenges associated with the use of three different electrophiles (aryl and alkyl halides and chloroformate) in multi-component cross-coupling reaction we decided to use density functional theory (D FT) calculations to better understand the details of the activation modes and the catalytic cycle (Figure 2). As a model reaction, we investigated the reaction of iodo-4-methoxybenzene (aryl iodide), ethyl chloroformate, and 7-bromoheptanenitrile (alkyl bromide) in the presence of Ni/phenanthroline as the active catalyst. The oxidative addition of electrophiles to a Ni^{I} intermediate is supported by recent mechanistic studies.[3–5] The reduction of Ni^{I} intermediate by zinc to form Ni^{0} intermediate was calculated to be thermodynamically unfavored (detailed discussion see Supporting Information 6.2). Therefore, we chose Ni^{I}-I (**A**) as the starting point of the catalytic cycle, which was generated from the reduction of NiI_2 by zinc. First, we investigated the oxidative additions of the three electrophiles to the intermediate **A**. The results showed that aryl iodide oxidative addition has the lowest energy barrier (**A-B1TS**, 11.0 kcal mol^{-1}), while the oxidative additions of ethyl chloroformate and alkyl bromide are significantly more difficult (ethyl chloroformate: **A-B2TS**, 21.2 kcal mol^{-1}; alkyl bromide: **A-B3TS**, 32.5 kcal mol^{-1}). The following comproportionation with another Ni^{I}-I (**A**) to form the Ni^{II} intermediate **B1**,[3a,4] which was further reduced by zinc to generate Ni^{I} intermediate **C** (detailed discussion about the Ni^{III} reduction, see Supporting Information 6.3). Here, we calculated the oxidative addition energy barriers of the three electrophiles again. It turned out that the oxidative addition of ethyl chloroformate had the lowest barrier (**C-D1TS**, 13.4 kcal mol^{-1}), while those of the other two electrophiles (alkyl bromide and aryl iodide) had higher energy barriers (alkyl bromide: **C-D2TS**, 23.8 kcal mol^{-1}; aryl iodide: **C-D3TS**, 26.7 kcal mol^{-1}). The formed Ni^{III} intermediate **D1** cannot undergo OEt-group migration because of the very high energy barrier (**D1-ETS**, 31.2 kcal mol^{-1}). However, **D1** can be reduced by zinc, and the following OEt-group migration gives Ni^{II} intermediate **F**. Interestingly, the OEt-group migration energy barrier is considerably lower for the Ni^{II}-complex (**F-GTS**, 25.6 kcal mol^{-1}) and Ni^{II} intermediate **G** is formed which subsequently is reduced again by the zinc to give Ni^{I} species **H**. Again, the oxidative additions of three electrophiles were evaluated for the 3rd time. Interestingly, the halogen abstraction of alkyl bromide is the easiest step (**H-I1TS**, 17.5 kcal mol^{-1}), while the other two electrophiles undergo oxidative addition with a higher energy barrier (ethyl chloroformate: **H-I2TS**, 23.2 kcal mol^{-1}; aryl iodide: **H-I3TS**, 26.8 kcal mol^{-1}). The generated Ni^{I} **I1** intermediate underwent CO migration via transition state **I1-JTS** (4.3 kcal mol^{-1}), followed by the radical addition to give the Ni^{III} intermediate **K**. Finally, reductive elimination afforded the aryl-alkyl ketone product and regenerated the active catalyst **A2**. The Ni^{I}-Br intermediate **A2** behaves very similarly to the initial Ni^{I}-I intermediate **A**.

However, the oxidative additions of three different electrophiles to **A2** were also investigated, and the results are similar (see Supporting Information).

Based on the above DFT calculations, a plausible catalytic cycle is shown in Figure 3.

According to the DFT studies, the Ni^{II} precatalyst is reduced to Ni^{0} by zinc, followed by comproportionation with Ni^{II} to generate the Ni^{I}-I **A**. Then, aryl iodide undergoes oxidative addition with the Ni^{I} intermediate **A**, followed by comproportionation with another Ni^{I} **A** to afford the Ar-Ni^{II}-I intermediate **B1**. The aryl iodide can undergo oxidative addition with Ni^{0}, which is an alternative way to generate intermediate **B1** in the initial catalytic cycle.[13] The resulting **B1** is further reduced by zinc to generate an Ar-Ni^{I} intermediate **C**. Oxidative addition of ethyl chloroformate with the Ar-Ni^{I} intermediate **C** gives a Ni^{III} intermediate **D1** which is reduced by zinc to furnish a Ni^{II} intermediate **F**. Upon OEt-group migration, a new Ni^{II} intermediate **G** is formed, followed by further reduction by zinc to offer an Ar-Ni^{I}-CO intermediate **H**. The halogen abstraction between intermediate **H** and alkyl bromides delivers the alkyl radical along with the intermediate **I1**. The CO migration takes place with the intermediate **I1** and forms the key intermediate **J**. Then, the alkyl radical is trapped by intermediate **J** to form the alkyl-Ni^{III}-acyl intermediate **K**, which undergoes reductive elimination to release the final product and regenerate the Ni^{I} species.

In line with the DFT calculation is the experimentally tested Ni-catalyzed reductive cross electrophile coupling with 1-bromo-3-phenylpropane (**1**), ethyl chloroformate (**2**) and 4- iodobenzoic acid methyl ester (**3a**) (Table 1). After experimentation, the desired ketone (**4a**) was obtained in 77 % isolated yield when a 1:2:2 ratio of **1**/**2**/**3a** was used along with NiI_2 as catalyst, 1,10-phenanthroline as ligand, Zn as reductant and $MgCl_2$ as additive in DMA (1.5 mL) as solvent (Table 1, entry 1). Control experiments revealed that NiI_2, 1,10-phenanthroline, and Zn all were crucial for the transformation, and no product was observed in their absence (entry 2, 4, 6). With the preformed nickel catalyst, 72 % yield was achieved (entry 3). Without $MgCl_2$, the reaction yield decreased (entry 5). The role of $MgCl_2$ in the process was attributed to the activation of Zn.[14] Replacing Zn with Mn led to 33 % yield (entry 7). Without ClCOOEt, no carbonylative coupling product was detected (entry 8). The yield was 66 % with 4-bromobenzoic acid methyl ester instead of 4-iodobenzoic acid methyl ester (**3a**) (entry 9).

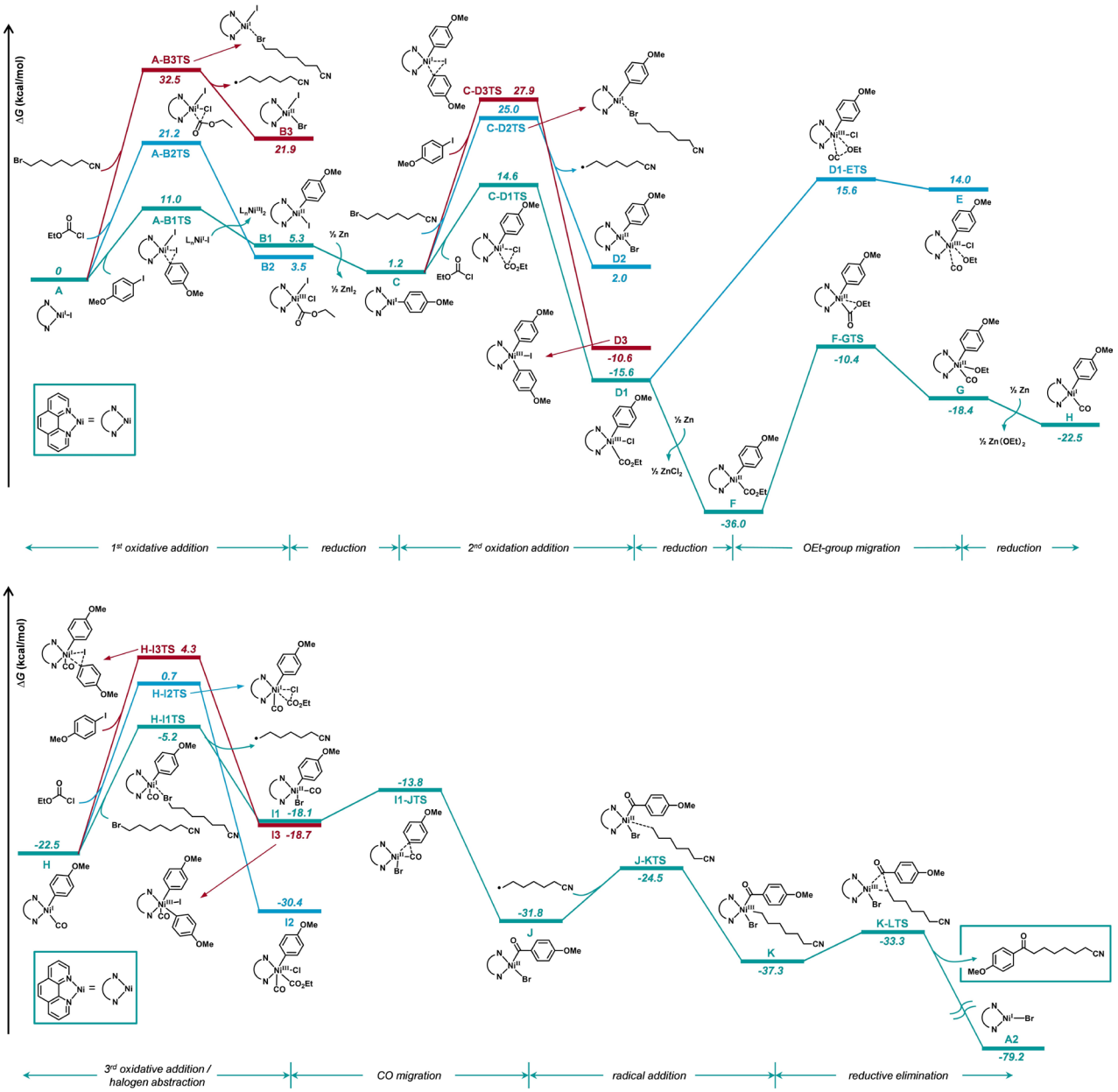

Figure 2. DFT-computed energy profiles of the catalytic cycle. Free energies in solution (in kcal mol^{-1}) calculated at SMD (DMA)-M06/Def2-TZVPP//PBE/Def2-TZVP (Ni, Zn)/Def2-SVP (other atoms).

Lowering the catalyst/ligand loading resulted in reduced yield (entry 10). The reaction can be scaled up, and 70 % yield was obtained with 2.0 mmol of **1** (entry 11).

With the optimized conditions in hand, we evaluated the scope of aryl iodides by reacting them with 1-bromo-3-phenylpropane (**1**), and ethyl chloroformate (**2**) (Figure 4a). This method shows excellent compatibility for a broad range of aryl iodides, and the corresponding products were isolated in moderate to excellent yields. Iodobenzenes bearing electron-neutral substituents (**4b** and **4c**) and electron-withdrawing substituents including ester, cyano, ketone, fluoro-, chloro-, and trifluoromethyl (**4a**, **4d**–**h**) furnished the corresponding products with moderate to good yields. Iodobenzenes bearing electron-donating substituents reacted more efficiently in the nickel catalyzed carbonylation protocol. With *para*- and *meta*-methoxyl substituted iodobenzenes, 92 % (**4i**) and 77 % (**4j**) isolated yields were obtained, respectively. The *ortho*-methoxyl substituted iodobenzene resulted in a lower coupling yield (42 %, **4k**), presumably due to increased steric hindrance. Methyl, *t*-butyl, methylthiomoieties, boronic esters, phenyl, and trifluoromethoxyl functional groups were well-tolerated

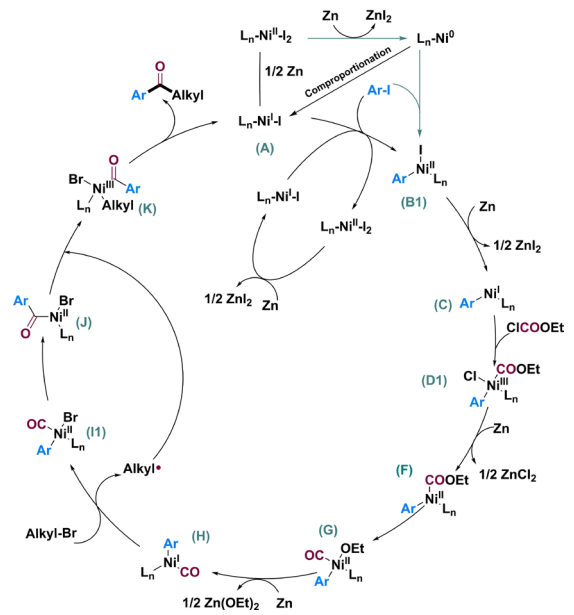

Figure 3. A proposed mechanism for catalytic carbonylation with nickel catalysis.

Table 1: Optimization for the three components carbonylation reaction.

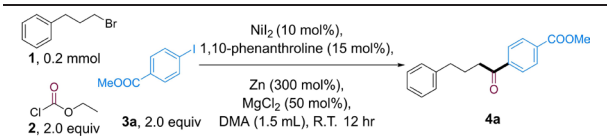

Entry	Variation from standard conditions[a]	Yield [%][b]
1	Standard conditions	77
2	w/o NiI_2	ND
3	Preformed catalyst	72
4	w/o 1,10-phenanthroline	ND
5	w/o $MgCl_2$	<10
6	w/o Zn	ND
7	Mn instead of Zn	33
8	w/o ClCOOEt	ND
9	4-bromobenzoic acid methyl ester	66
10	5 mol% NiI_2, 7.5 mol% ligand	31
11	**1** in 2.0 mmol	70%

[a] Standard conditions: **1** (0.2 mmol), **2** (2.0 equiv), **3a** (2.0 equiv), NiI_2 (10 mol%), 1,10-phenanthroline (15 mol%), Zn (3.0 equiv), $MgCl_2$ (50 mol%), DMA (dimethylacetamine, 1.5 mL), room temperature, 12 hours. [b] Isolated yield.

ORCID ID for the authors:

(**4l–r**). D isubstituted iodobenzene (**4s**) also reacted with good efficiency. N-Boc-5-iodoindole and 4-Iodo-2-methoxypyridine could give the desired products (**4t**, **4u**) in moderate yields. It should be noted that fluoro, chloro, and boronic esters groups were tolerated, providing opportunities for further functionalization. To further illustrate the utility of this carbonylation strategy, we sought to integrate the carbonylation approach into the diversification of complex molecules; carbonyls were subsequently installed into various pharmaceutically-relevant heterocyclic substrates containing thiophene (**5**), furan (**6**), phthalimidyl (**10**), 5-Norbornene-2- carboxylic acid (**8**), commercial drug derivative (**9**, from Ibuprofen), and natural products (**11**, from (+)-δ-Tocopherol and **7**, from geranic acid) in reasonably good to excellent yields.

The carbonylation protocol also displayed good compatibility across a range of primary and secondary alkyl halides. As shown in Figure 4b, when benzyl chloride was introduced, product **12** was isolated in 69% yield. Primary alkyl bromides were also active, and the length of the carbon chains had almost no influence on the reaction efficiency (**13–15**). Both electron-withdrawing and electron-donating groups on the aromatic rings were tolerated (**16–18**). Simple alkyl bromides, such as 1-bromobutane (**19**), furnished the desired product in good yield.

Functional groups such as alkene, chloro, cyano, ether, ester, *t*- butyl-dimethylsilane ether, and phthalimidyl were all well tolerated (**20–26**). Secondary alkyl bromides yielded trace amount of ketone, whereas secondary alkyl iodides resulted in moderate yields in the presence of Ni $(COD)_2$ catalyst (**27–30**). Notably, the activated alkane 2-chloropropionate could give the desired ketone in 62% yield (**31**) with (*R*)-4-(*tert*-butyl)-2-(pyrimidin-2-yl)-4,5-dihydrooxazole as ligand. We also tried the reaction with *tertiary* alkyl halides. Unfortunately, only a trace amount of product could be detected (see Figure S5).

In addition, we conducted the reaction of the organozinc reagent (**1a**) with **2** and methyl 4-iodobenzoate under the standard condition (Figure 5a), and no desired ketone product was observed, indicating that the formation of ketones is not occurring via an in situ formed organozinc reagent.

The activation of alkyl halides typically leads to radical intermediates.[15] To confirm the alkyl radicals involved in this protocol, we performed a series of control experiments. We first introduced 2.0 equiv TEMPO into the reaction mixture under standard conditions. The reaction was inhibited completely, and compound **32** was obtained in 37% yield (Figure 5b). The control experiments in Figure S4 reveal that the presence of both Ni catalyst and zinc powder were essential for the activation of alkyl bromide. Also, the use of bromomethyl cyclopropane (**33**) failed to offer the desired ketone, but instead furnished a ring-opened product (**20**) (Figure 5c). The coupling of alkyl bromide **34** with ethyl chloroformate and 4-methoxyiodobenzene furnished the cyclization/coupling product **35** in 30% yield (Figure 5d). All of these results support the involvement of an alkyl radical in this transformation.[16] To validate the oxidative addition sequences proposed by the DFT studies, a series of sequential reactions were performed (Figure S6), which are in line with the DFT studies and demonstrate that the three electrophiles undergo reaction in the order aryl iodide, chloroformate, and alkyl bromide.

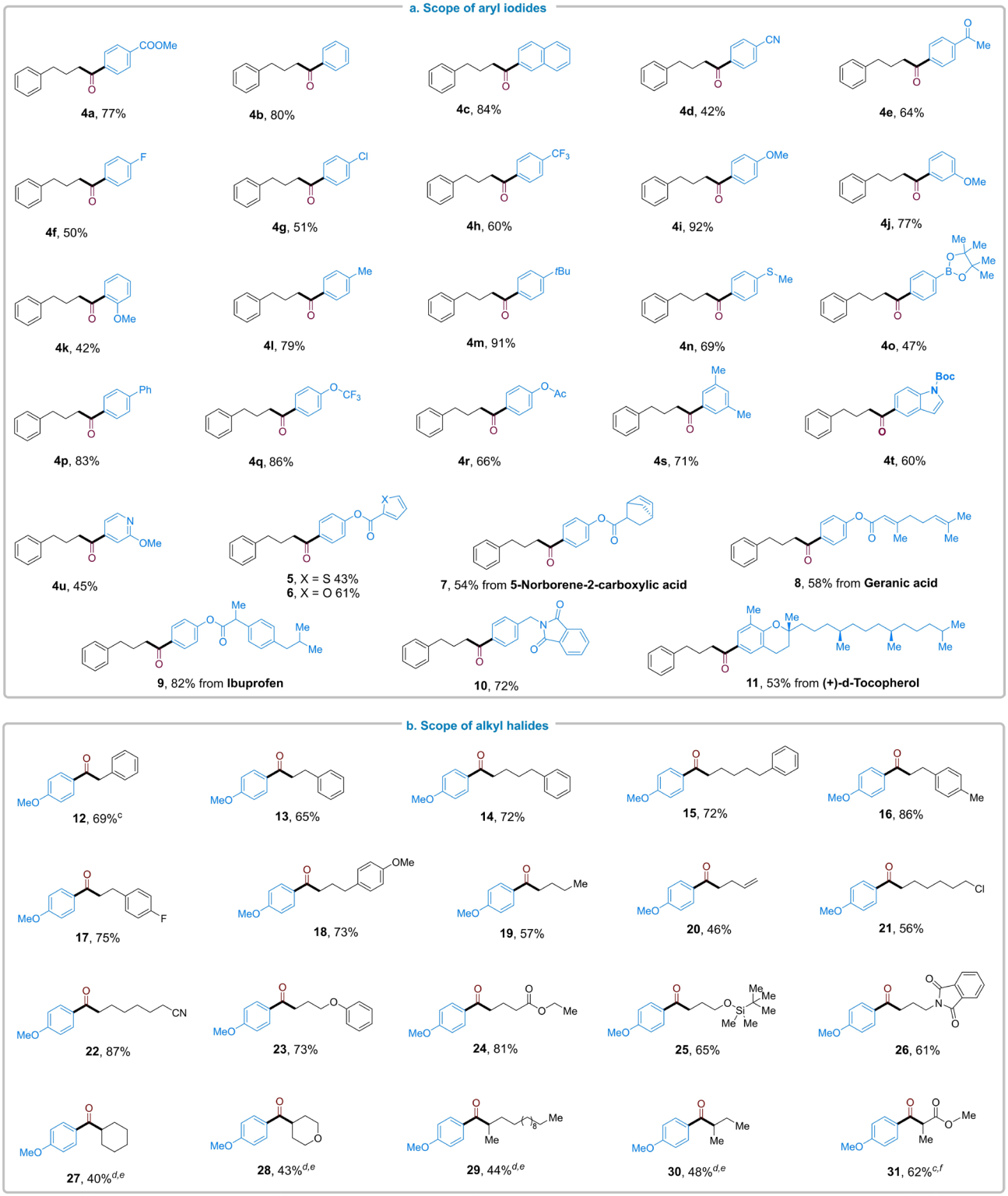

Figure 4. a) Scope of aryl iodides and b) scope of alkyl halides. [a] The reaction was carried out with **1** (0.2 mmol), **2** (2.0 equiv), **3** (2.0 equiv), NiI_2 (10 mol%), 1,10-phenanthroline (15 mol%), $MgCl_2$ (50 mol%), Zn (3.0 equiv) and DMA (1.5 mL), room temperature, 12 hours. [b] Isolated yield. [c] Alkyl-Cl was used. [d] Alkyl-I was used. [e] Ni $(COD)_2$(10 mol%). [f] (*R*)-4-(*tert*-butyl)-2-(pyrimidin-2-yl)-4,5-dihydrooxazole as ligand.

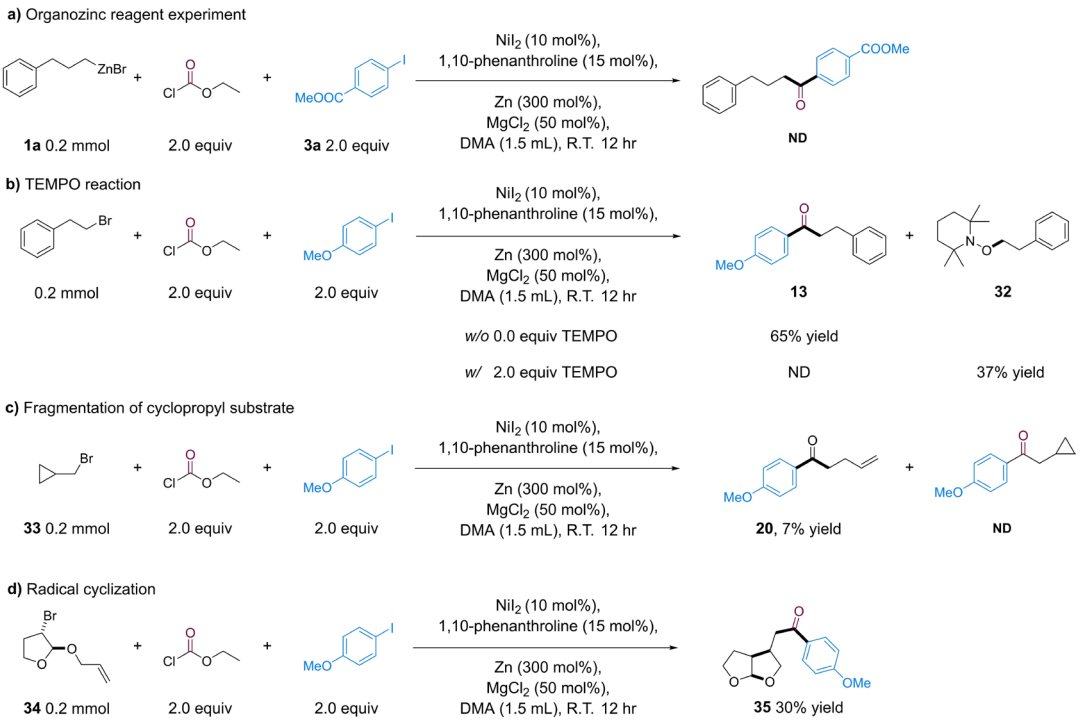

Figure 5. Mechanistic experiment. a) Organozinc reagent experiment. b) TEMPO capture reaction. c) Fragmentation of cyclopropyl substrate. d) Radical cyclization reaction. The yield was detected by GC (FID).Haifeng Chen: 0000-0002-1702-6771

Conclusion

In conclusion, we report a nickel catalyzed reductive carbonylation strategy to synthesize a wide range of aryl-alkyl ketones (49 examples) from commercially available alkyl halides, aryl halides, and ethyl chloroformate as a safe and effective carbonyl replacement. This mild carbonylation protocol has a broad scope and high functional group tolerance, and provides an efficient and practical alternative strategy for the synthesis of aryl-alkyl ketones. DFT calculations and experimental findings provide new insight into the complex reaction sequence involving three different electrophiles and demonstrate that the sequence of oxidative additions starts with the aryl halide, followed by ethyl chloroformate, and finally alkyl bromide. This knowledge should be useful for synthesis planning and the further development of multi-component cross-coupling reactions.

Acknowledgements

This work was financially supported by the King Abdullah University of Science and Technology (KAUST), Saudi Arabia, Office of Sponsored Research (URF/1/4405). The authors acknowledge the KAUST Supercomputing Laboratory for providing the computational resources of the Shaheen-II supercomputer.

Conflict of Interest

The authors declare no conflict of interest.

Data Availability Statement

The data that support the findings of this study are available in the Supporting Information of this article.

Keywords: Alkyl Halides · Aryl Halides · Carbonylation · Ethyl Chloroformate · Nickel

[1] a) S. Z. Tasker, E. A. Standley, T. F. Jamison, *Nature* **2014**, *509*, 299–309; b) D. A. Everson, D. J. Weix, *J. Org. Chem.* **2014**, *79*, 4793–4798; c) D. J. Weix, *Acc. Chem. Res.* **2015**, *48*, 1767–1775; d) J. Gu, X. Wang, W. Xue, H. Gong, *Org. Chem. Front.* **2015**, *2*, 1411–1421; e) A. H. Cherney, N. T. Kadunce, S. E. Reisman, *Chem. Rev.* **2015**, *115*, 9587–9652; f) X. Wang, Y. Dai, H. Gong, *Top. Curr. Chem.* **2016**, *374*, 43; g) J. Choi, G. C. Fu, *Science* **2017**, *356*, eaaf7230; h) G. C. Fu, *ACS Cent. Sci.* **2017**, *3*, 692–700; i) E. L. Lucas, E. R. Jarvo, *Nat. Chem. Rev.* **2017**, *1*, 0065; j) "Cross Electrophile Coupling: Principles and New Reactions": M. J. Goldfogel, L. Huang, D. J. Weix in *Nickel Catalysis in Synthesis: Methods and Reactions, Vol. 352* (Ed.: S. Ogoshi), Wiley-VCH, Weinheim, **2020**, pp. 183–222; k) J. Liu, Y. Ye, J. L. Sessler, H. Gong, *Acc. Chem. Res.* **2020**, *53*, 1833–1845; l) W. Xue, X. Jia, X. Wang, X. Tao, Z. Yin, H. Gong, *Chem. Soc. Rev.* **2021**, *50*, 4162–4184; m) C. Zhu, H. Yue, J. Jia, M. Rueping, *Angew. Chem. Int. Ed.* **2021**, *60*, 17810–17831; *Angew. Chem.* **2021**, *133*, 17954–17975; n) L. Yi,

T. Ji, K.-Q. Chen, X.-Y. Chen, M. Rueping, *CCS Chem.* **2022**, *4*, 9–30.

[2] a) X. Hu, *Chem. Sci.* **2011**, *2*, 1867–1886; b) V. P. Ananikov, *ACS Catal.* **2015**, *5*, 1964–1971; c) J. B. Diccianni, T. Diao, *Trends Chem.* **2019**, *1*, 830–844.

[3] a) Q. Lin, T. Diao, *J. Am. Chem. Soc.* **2019**, *141*, 17937–17948; b) J. Diccianni, Q. Lin, T. Diao, *Acc. Chem. Res.* **2020**, *53*, 906–919; c) Q. Lin, Y. Fu, P. Liu, T. Diao, *J. Am. Chem. Soc.* **2021**, *143*, 14196–14206.

[4] S. I. Ting, W. L. Williams, A. G. Doyle, *J. Am. Chem. Soc.* **2022**, *144*, 5575–5582.

[5] N. A. Till, S. Oh, D. W. C. MacMillan, M. J. Bird, *J. Am. Chem. Soc.* **2021**, *143*, 9332–9337.

[6] R. Shi, X. Hu, *Angew. Chem. Int. Ed.* **2019**, *58*, 7454–7458; *Angew. Chem.* **2019**, *131*, 7532–7536.

[7] a) A. Rérat, C. Michon, F. Agbossou-Niedercorn, C. Gosmini, *Eur. J. Org. Chem.* **2016**, 4554–4560; b) J. Chen, S. Zhu, *J. Am. Chem. Soc.* **2021**, *143*, 14089–14096.

[8] a) R. K. Dieter, *Tetrahedron* **1999**, *55*, 4177–4236; b) N. J. Lawrence, *J. Chem. Soc. Perkin Trans. 1* **1998**, 1739–1749; c) J. Singh, N. Satyamurthi, I. J. Aidhen, *Prakt. Chem.* **2000**, *342*, 340–347; d) J. R. Luque-Ortega, P. Reuther, L. Rivas, C. Dardonville, *J. Med. Chem.* **2010**, *53*, 1788–1798; e) S. K. Vooturi, C. M. Cheung, M. J. Rybak, S. M. Firestine, *J. Med. Chem.* **2009**, *52*, 5020–5031.

[9] A. H. Cherney, N. T. Kadunce, S. E. Reisman, *J. Am. Chem. Soc.* **2013**, *135*, 7442–7445.

[10] a) M. Medio-Simón, C. Mollar, N. Rodriguez, G. Asensio, *Org. Lett.* **2005**, *7*, 4669–4672; b) J. Sävmarker, J. Lindh, P. Nilsson, *Tetrahedron Lett.* **2010**, *51*, 6886–6889; c) X. F. Wu, H. Neumann, M. Beller, *Tetrahedron Lett.* **2010**, *51*, 6146–6149; d) A. K. Steib, T. Thaler, K. Komeyama, P. Mayer, P. Knochel, *Angew. Chem. Int. Ed.* **2011**, *50*, 3303–3307; *Angew. Chem.* **2011**, *123*, 3361–3365.

[11] Examples: a) A. Brennführer, H. Neumann, M. Beller, *Angew. Chem. Int. Ed.* **2009**, *48*, 4114–4133; *Angew. Chem.* **2009**, *121*, 4176–4196; b) X. F. Wu, H. Neumann, M. Beller, *Chem. Soc. Rev.* **2011**, *40*, 4986–5009; c) Q. Liu, H. Zhang, A. Lei, *Angew. Chem. Int. Ed.* **2011**, *50*, 10788–10799; *Angew. Chem.* **2011**, *123*, 10978–10989; d) S. Sumino, T. Ui, I. Ryu, *Org. Lett.* **2013**, *15*, 3142–3145; e) C. Brancour, T. Fukuyama, Y. Mukai, T. Skrydstrup, I. Ryu, *Org. Lett.* **2013**, *15*, 2794–2797; f) J. B. Peng, B. Chen, X. Qi, J. Ying, X. F. Wu, *Adv. Synth. Catal.* **2018**, *360*, 4153–4160; g) H. Zhao, B. Hu, L. Xu, P. J. Walsh, *Chem. Sci.* **2021**, *12*, 10862–10870; h) Y. Yuan, F. Zhao, X. F. Wu, *Chem. Sci.* **2021**, *12*, 12676–12681; i) Y. Wu, L. Zeng, H. Li, Y. Cao, J. Hu, M. Xu, R. Shi, H. Yi, A. Lei, *J. Am. Chem. Soc.* **2021**, *143*, 12460–12466.

[12] Examples: a) A. C. Wotal, D. J. Weix, *Org. Lett.* **2012**, *14*, 1476–1479; b) H. Yin, C. Zhao, H. You, K. Lin, H. Gong, *Chem. Commun.* **2012**, *48*, 7034–7036; c) F. Wu, W. Lu, Q. Qian, Q. Ren, H. Gong, *Org. Lett.* **2012**, *14*, 3044–3047; d) A. C. Wotal, R. D. Ribson, D. J. Weix, *Organometallics* **2014**, *33*, 5874–5881; e) C. E. I. Knappke, S. Grupe, D. Gärtner, M. Corpet, C. Gosmini, A. J. von Wangelin, *Chem. Eur. J.* **2014**, *20*, 6828–6842; f) X. Jia, X. Zhang, Q. Qian, H. Gong, *Chem. Commun.* **2015**, *51*, 10302–10305; g) L. Fan, J. Jia, H. Hou, Q. Lefebvre, M. Rueping, *Chem. Eur. J.* **2016**, *22*, 16437; h) X. Liu, C. Hsiao, L. Guo, M. Rueping, *Org. Lett.* **2018**, *20*, 2976–2979; i) A. Chatupheeraphat, H. H. Liao, W. Srimontree, L. Guo, Y. Minenkov, A. Poater, L. Cavallo, M. Rueping, *J. Am. Chem. Soc.* **2018**, *140*, 3724–3735; j) P. E. Krach, A. Dewanji, T. Yuan, M. Rueping, *Chem. Commun.* **2020**, *56*, 6082–6085; k) D. Mazzarella, A. Pulcinella, L. Bovy, R. Broersma, T. Noël, *Angew. Chem. Int. Ed.* **2021**, *60*, 21277–21282; *Angew. Chem.* **2021**, *133*, 21447–21452.

[13] S. Bajo, G. Laidlaw, A. R. Kennedy, S. Sproules, D. J. Nelson, *Organometallics* **2017**, *36*, 1662–1672.

[14] For the role of $MgCl_2$ additive, see: a) C. Zhao, X. Jia, X. Wang, H. G. Gong, *J. Am. Chem. Soc.* **2014**, *136*, 17645–17651; b) X. Wang, G. Ma, Y. Peng, C. E. Pitsch, B. J. Moll, T. D. Ly, X. Wang, H. Gong, *J. Am. Chem. Soc.* **2018**, *140*, 14490–14497; c) Y. Ye, H. F. Chen, J. L. Sessler, H. G. Gong, *J. Am. Chem. Soc.* **2019**, *141*, 820–824; d) L. Huang, L. K. G. Ackerman, K. Kang, A. M. Parsons, D. J. Weix, *J. Am. Chem. Soc.* **2019**, *141*, 10978–10983.

[15] a) C. Amatore, A. Jutand, J. Perichon, Y. M. Rollin, *Chem* **2000**, *131*, 1293–1304; b) S. Biswas, D. J. Weix, *J. Am. Chem. Soc.* **2013**, *135*, 16192–16197.

[16] a) D. A. Powell, T. Maki, G. C. Fu, *J. Am. Chem. Soc.* **2005**, *127*, 510–511; b) F. González-Bobes, G. C. Fu, *J. Am. Chem. Soc.* **2006**, *128*, 5360–5361; c) S. E. Creutz, K. J. Lotito, G. C. Fu, J. C. Peters, *Science* **2012**, *338*, 647–651; d) H. Chen, X. Jia, Y. Yu, Q. Qian, H. Gong, *Angew. Chem. Int. Ed.* **2017**, *56*, 13103–13106; *Angew. Chem.* **2017**, *129*, 13283–13286.

Manuscript received: March 20, 2022
Accepted manuscript online: June 21, 2022
Version of record online: July 11, 2022